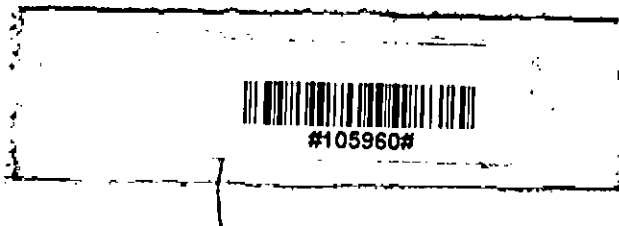


# STUDY OF A TWO-PHASE LOOPED THERMOSYPHON

BY

SWAPAN KUMAR SARKER



DEPARTMENT OF MECHANICAL ENGINEERING  
BANGLADESH UNIVERSITY OF ENGINEERING & TECHNOLOGY  
DHAKA-1000, BANGLADESH

## CERTIFICATE OF APPROVAL

The thesis titled" Study of a Two-Phase Looped Thermosyphon" submitted by Swapan Kumar Sarker, Roll No : 040310010F, Session April 2003 has been accepted as satisfactory in partial fulfillment of the requirement for the degree of M. Engineering in Mechanical Engineering.

### BOARD OF EXAMINERS



---

**Dr. Chowdhury Md. Feroz (Supervisor)**  
Professor  
Mechanical Engineering Department  
BUET, Dhaka.

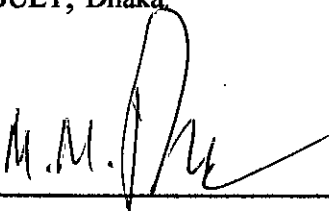
**Chairman**



---

**Dr. Abu Rayhan Md. Ali**  
Professor  
Mechanical Engineering Department  
BUET, Dhaka.

**Member**



---

**Dr. Muhammed Mahbubur Razzaque**  
Associate Professor  
Mechanical Engineering Department  
BUET, Dhaka.

**Member**

# CONTENTS

	<b>PAGES</b>
List of Tables	i
List of Figures	i
Nomenclatures	ii
Acknowledgement	iii
Abstract	iv

## TABLE OF CONTENTS:

### **CHAPTER 1 : INTRODUCTION**

1.1 Motivation	4
1.2 Objective	5

### **CHAPTER 2 : LITERATURE REVIEW**

2.1 The Early History	6
2.2 The Revolution	7
2.3 The Modern Trends	8

### **CHAPTER 3 : EXPERIMENTAL SET UP AND EXPERIMENTAL PROCEDURE**

3.1 Experimental Apparatus	9
3.2 Working fluids	11
3.3 Experimental procedure	13
3.4 Mathematical Equation	13

### **CHAPTER 4 : RESULTS AND DISCUSSION**

### **CHAPTER 5 : CONCLUSIONS**

### **APPENDIX : APPLICATION OF THERMOSYPHON**

**LIST OF TABLES****PAGES**

Table 1	:	The detail dimensions of thermosyphon	10
Table 2	:	Thermophysical properties of working fluids	12

**LIST OF FIGURES**

Figure 3.1.a		Dimensions of thermosyphon	14
Figure 3.1.b		Schematic diagram of thermosyphon	15
Figure 3.1.c		Experimental apparatus	16
Figure 4.1.1.1		Temperature distribution of thermosyphon for different heat flux with acetone as the working fluid	21-23
Figure 4.1.1.2		Temperature distribution of thermosyphon for different heat flux with ethanol as the working fluid	24-26
Figure 4.1.1.3		Temperature distribution of thermosyphon for different heat flux with methanol as the working fluid	27-29
Figure 4.1.1.4		Temperature distribution of thermosyphon for different heat flux with water as the working fluid	30-32
Figure 4.1.2.1		Temperature distribution of thermosyphon for different coolant flow rate with acetone as the working fluid	33-34
Figure 4.1.2.2		Temperature distribution of thermosyphon for different coolant flow rate with ethanol as the working fluid	35-36
Figure 4.1.2.3		Temperature distribution of thermosyphon for different coolant flow rate with methanol as the working fluid	37-38
Figure 4.1.2.4		Temperature distribution of thermosyphon for different coolant flow rate with water as the working fluid	39-40
Figure 4.2.1		Effect of coolant flow rate on thermal resistance	41-44
Figure 4.2.2		Effect of heat flux rate on thermal resistance	45-48
Figure 4.3.1		Effect of working fluid on thermal resistance	49
Figure 4.3.2		Effect of working fluid on overall heat transfer coefficient	50

---

## NOMENCLATURE

<u>Symbol</u>	<u>Meaning</u>	<u>Unit</u>
A	Surface area of evaporator	m <sup>2</sup>
m	Flow rate	l/min
Q	Input power	W
q	Heat flux	kW/m <sup>2</sup>
R	Thermal Resistance	°C/W
T	Temperature	°C
U <sub>t</sub>	Overall heat transfer coefficient	kW/m <sup>2</sup> °C

### Subscript

e	Evaporator
c	Coolant

---

## ACKNOWLEDGEMENTS

This author hereby wishes to express his heartiest and sincerest gratitude and indebtedness to **Dr. Chowdhury Md. Feroz**, Professor, Mechanical Engineering Department, Bangladesh University of Engineering and Technology, Dhaka, for his guidance, inspiration, constructive suggestions and close supervision throughout the entire period of the experimental investigation.

The author also express thankful gratitude to **Dr. Abu Rayhan Md. Ali** Professor, Mechanical Engineering Department, Bangladesh University of Engineering and Technology, Dhaka, **Dr. Muhammed Mahbubur Razzaque** , Associate Professor, Mechanical Engineering Department, Bangladesh University of Engineering and Technology, Dhaka, for their cooperation, valuable suggestion and inspiration for completion of this thesis.

A lot of thank are due for **Mr. Indrogit Roy**, Lab Attendant of Heat transfer Laboratory of Mechanical Department for his cooperation all through the research work. Thanks are also given especially to **Mr. Masudur Rahman**, Assistant Instrument Engineer, Mechanical Engineering Department, Bangladesh University of Engineering and Technology, Dhaka for his cooperation.

---

## ABSTRACT

The present experimental work investigates the heat transfer performance of looped parallel thermosyphon which consists of two single tube thermosyphon connected by two U tubes of same diameter at the top and bottom ends. For this purpose, the copper tube of 5.78 mm ID used with ethanol, methanol, acetone and water as the working fluid. Heat transfer characteristics are determined experimentally, based on the principle of phase change at different heat flux and different coolant flow rates. An analysis of the experimental data gives that the axial wall temperature of both condenser and evaporator sections decreases with the increase of coolant flow rate. The wall temperature increases with increase of heat flux. The thermal resistance decreases with the increase of both coolant flow rate and thermal load. Overall heat transfer coefficient increases with the increase of both coolant flow rate and heat flux. Among the working fluids used in the present study, ethanol shows the best performance.



## INTRODUCTION

### 1.1 MOTIVATION

Thermosyphon or heat pipe is a device of very high thermal conductance. Among other cooling technique heat pipe emerged as the most appropriate technology and cost effective thermal design due its excellent heat transfer capacity, high efficiency and structural simplicity. The heat pipe can, even in its simplest form, provide a unique medium for the study of several aspects of fluid dynamics and heat transfer, and it is growing in significance as a tool for use by the practicing engineer or physicist in applications ranging from heat recovery to precise control of laboratory experiments.

The idea of looped parallel thermosyphon (1) (2) is developed to minimize several insufficient performances of single tube thermosyphon such as low maximum heat transfer rate and non-uniform wall temperature in an evaporator section. In LPT, two single type thermosyphons are joined by two U-tubes at the top and bottom ends and thus total heat transfer area is increased. A small quantity of fluid is placed in the tube from which the air is evacuated and the tube sealed. The lower end of the tube (evaporator section) is heated causing the liquid to vaporize the vapor to move to the cold end of the tube (condenser section) where it is condensed. The condensate is returned to the hot end by gravity. Since the latent of evaporation is large, considerable quantities of heat can be transported.

Thermal designers have widely accepted the miniature looped parallel thermosyphon (MLPT) for their thermal design solution and the area of application is increases day by day. Normally MLPTs have 3 to 6 mm diameter and less than 400 mm length. Most preferable length is 150 mm. MLPT is relatively a new technology; relevant data, information is quite scarce (3). So, a thorough investigation of heat transfer capability of MLPT is indispensable for further development and improvement of performance. The applications of thermosyphon are given in Appendix. The purposes of this study are to show heat transfer characteristics in evaporator and condenser sections in miniature looped parallel thermosyphon (MLPT) and experimentally examined the maximum heat transfer rate, wall temperature profile and thermal resistance in the test sections.



## **1.2 OBJECTIVES**

The specific objectives of this study are to

- (a) To study the heat transfer performance of looped thermosyphon varying heat flux in the evaporator.
- (b) To analyze the heat transfer performance of looped thermosyphon.
- (c) To study the performance of looped thermosyphon varying the flow of coolant in the condenser.
- (d) To study the effect of working fluids on the performance of thermosyphon.

### LITERATURE REVIEW

In recent years, thermosyphon used for heat dissipation and homogenous temperature of computer and numerous electronic instruments has displayed its remarkable effect. So a through investigation on thermosyphon is indispensable for further development and improvement of its performance.

#### 2.1 THE EARLY HISTORY

*E. Schmidt*, a German engineer, first conducted experiments on heat pipe. He reported that a copper tube filled with ammonia or carbon dioxide near its critical point transfers an amount of heat per unit time that is more than 4000 times larger than that of a solid rod of copper with same dimensions and at the same temperature difference between the hot and cold regions. But the limitation of that experiment is that it can operate only in a vertical position.

RCA, the first commercial organization that worked on heat pipe, using glass, copper, nickel, stainless steel, and molybdenum as tube materials. Working fluid included water, cesium, sodium, lithium, and bismuth. Maximum operating temperature of 1650°C had been achieved.

Heat pipe was first used in space for satellite thermal control on GEOS-B, launched from Vandenberg Air Force base. The purpose of the heat pipe was to minimize the temperature difference between the various transponders in the satellite [4].

NASA developed a new type of heat pipe (rotating heat pipe) in which the wick was omitted. These heat pipes were utilized for cooling motor rotors and turbine blade rotors.

The Rutherford High Energy Laboratory was the first organization in UK to operate cryogenic heat pipes. These heat pipes were used for cooling detector in satellite infrared scanning systems.

A wide variety of heat pipes were commercially available from a number of companies in the United States. RCA, Thermo-Electron and Noren Products were among several firms marketing a

range of 'standard' heat pipes, with the ability to construct 'special' for specific customer applications. During the next few years several manufacturers were established in the United Kingdom and a number of companies specializing in heat pipes heat recovery systems.

## 2.2 THE REVOLUTION

*Boman* at the McDonnell Douglas Aircraft Company tested a Hastelloy X-sodium heat pipe for use on the wing leading edge of an advanced re-entry vehicle. *Glass* at the NASA Langley Research Center presented a thermal analysis of a carbon-carbon/refractory-metal heat-pipe-cooled wing leading edge.

*Merrigan* at Los Alamos National Laboratory tested aluminaborosilicate-covered stainless steel-sodium heat pipes to use in high temperature radiators. The tests indicated radiation heat rejection rates from the fabric-covered surface was strongly affected by the emittance of the underlying metal substrate. In the same year, *Ranken* at Los Alamos National Laboratory presented the results of studies on a thermionic reactor concept that uses a combined beryllium and zirconium hydride moderator, allows heat pipe, cooling of a compact thermionic fuel element.

*Gottschlich* at Wright-Patterson Air Force Base described the cooling of gas turbine engine vanes using heat pipes. A heat pipe flight test was on a Hitchhiker canister aboard the Space Shuttle Discovery (STS-53) . The canister housed two oxygen heat pipe designs: one made by TRW in Torrance, California, the other by Hughes Aircraft Company in Huntington Beach, California. These heat pipes, cooled by five Stirling-cycle cryocoolers, were developed to demonstrate heat rejection techniques for spacecraft infrared sensors.

*Woloshun* described the design, fabrication, and ground test at Los Alamos National Laboratory of three stainless steel-potassium heat pipes: one with a homogeneous screen wick, one with an arterial wick, and the last with an annular gap wick. This experiment, sponsored by the US Air Force Phillips Laboratory, flew aboard STS-77 becoming the first American-built liquid metal heat pipes to operate in micro gravity conditions.

*McDonald* at Martin Marietta described a pair of copper-acetone heat pipes built by Thermacore. These heat pipes were designed to transfer heat from a refrigerated space to the cold finger of a Stirling-cycle cooler.

*Judd* investigated the use of heat pipes to regulate the temperature of a carbide cutting tool on an engine lathe. Acrolab, incorporated in Windsor, Ontario manufactures heat pipes to isothermalize molds and extruders used in the plastics and rubber industries.

## 2.3 THE MODERN TRENDS

A breakthrough innovation in the application of heat pipe technology in modern times came through the miniaturization of heat pipes. Studies on the application of miniature heat pipes having the diameter of 3 or 4 mm for cooling of the notebook PC CPU have been actively conducted by the American and Japanese enterprises specializing in heat pipes recently [5][6][7]. *Kwang Soo Kim, et. al.* [8] performed an experimental investigation on cooling characteristics of miniature heat pipes having the same dimension [3 or 4 mm] with woven wired wick and water as a working fluid. The experimental parameters of their experiment were inclination, structure of the wick and length of the condenser. They claimed that the heat transfer rate increases with the increasing condenser length. *Jian Ling et. al.*, [9] experimentally investigated on radially rotating miniature high-temperature heat pipes. The experimental parameters were input power, diameter and coolant flow rate. The experimental data prove that the radially rotating miniature high-temperature heat pipe has a high effective thermal conductance, which is 60–100 times higher than the thermal conductivity of copper, and a large heat transfer capacity that is more than 300 W. *Lanchao Lin et. al.* [10] experimentally investigated on high performance miniature heat pipes with new capillary structure –notched fins, capillary fins and flooded sheet fins. They predicted that the heat pipe with notched fins has the lowest internal thermal resistance at similar operating temperatures. *Amir Faghri et. al.* [11] experimentally and mathematically found that the flat miniature heat pipes are easily capable of withstanding heat fluxes on the order of 40 w/ sq cm on the evaporator wall. *Jun Zhuang et. al.* [12] have carried out test and comparison to the starting performance, maximum transfer power and heat transfer performance under condition of antigravity of the miniature heat pipes with three different structural wicks (sintered, mesh and fiber). They found that all structures of wicks have little influence on the heat transfer capability of miniature heat pipe with the aid of gravity. Under condition of antigravity, the structure of wicks has obvious influence on the heat transfer capability of miniature heat pipes. *Thang Nguyen et. al.* [13] experimentally investigated on “Prediction of long-term performance of Miniaturc Heat Pipe from Accelerated Life tests”. Ignoring effect of non-condensable gases they have carried out the life tests at elevated temperature of 40, 70, 100, 130°C for over 350 days. They predicted that the heat pipe will degrade about 5°C over 15 years under the operating temperature of 70°C.

## EXPERIMENTAL METHODS

In order to study the heat transfer characteristics of looped thermosyphon, an experimental facility has been designed, fabricated and installed. The detailed description of experimental apparatus and experimental procedure are presented in the subsequent sections of this chapter.

### 3.1 EXPERIMENTAL APPARATUS

The experimental apparatus are as follows:

- a. Looped thermosyphon
- b. Test stand
- c. Heating apparatus
  - i. Power supply unit
  - ii. Ni-Cr thermic wire
- d. Cooling apparatus
  - i. Elevated water tank
  - ii. Flowmeter
- e. Measuring apparatus
  - i. Digital thermometer
  - ii. Thermocouple wire
  - iii. Selector switch

### 3.1.a. Looped thermosyphon

The schematic diagram of experimental apparatus is shown in the fig-3.1.c. The test loop consists of a pair of evaporator, adiabatic, condenser and U tube sections and is vertically oriented. Detailed dimensions of the MLPT are shown in the fig-3.1.b. Two evaporator and two condenser sections are located at bottom and top of the loop, respectively. All sections are made of 5.78 mm ID copper tube. The length of the evaporator, adiabatic, and condenser sections are 50 mm, 30 mm, and 70 mm, respectively. The both tubes are connected by U tubes with the same inside diameter at top and the bottom. The U tube is a half of a circular ring with 31.72 mm inner radius .

Two single tube thermosyphon consists of three sections are as shown in figure 3.1.a.

- i. Evaporator section
- ii. Adiabatic section
- iii. Condenser section

The detail dimension of Looped thermosyphon used in the experiment is summarized in Table-1.

**Evaporator section:** It is bottom part of thermosyphon. Heat is added to the thermosyphon through evaporator section.

**Condenser section:** It is upper most part of the thermosyphon. Heat is removed from the thermosyphon through condenser section.

**Adiabatic section:** Adiabatic section is located in between the evaporator and condenser section. This section is actually kept with heat pipe to distinguish evaporator section and condenser section. Adiabatic section is thermally insulated.

**Table 1: The detail dimension of thermosyphon**

Parameters	Dimension (mm)
Outside diameter of pipe, $d_o$	6.48
Inside diameter of pipe, $d_i$	5.78
Length of evaporator, $L_e$	50
Length of adiabatic section, $L_a$	30
Length of condenser, $L_c$	70

### 3.1. b. Test stand

It is a wooden stand. It is used for supporting thermosyphon.

### 3.1. c. i. Power supply unit

A DC power supply unit (Model: GPC 1850, Made in Malaysia) having voltage range 0~30 V and current range 0~3 Amp is used.

**3.1. c. i. Ni-Cr wire :** Ni-Cr thermic wire having diameter of 0.28 mm (10  $\Omega$ /m) are wound around the wall of the evaporator at a constant interval of 1.5 mm. To prevent electric contact, mica sheet is placed between thermic wire and copper tube.

### **3.1. d. i. Elevated water tank**

A water tank, mounted at about 10 feet height is used to supply cooling water to the condenser section.

### **3.1. d. i i. Flowmeter**

To control the flow of cooling water to the condenser, a flow meter (Made in USA, Capacity: 0~1 l/min ) is used.

### **3.1. e. i. Digital thermometer**

A digital thermometer (TM: OMEGA, Made in USA) is used to measured the wall temperature at various points on thermosyphons.

### **3.1. e. i i. Thermocouple**

Eight calibrated thermocouples of T type ( $\Phi= 0.18\text{mm}$ ) are glued to the wall of the thermosyphon four units at the evaporator section, two units at the adiabatic section, and two units at the condenser section.

### **3.1. e. i i i. Selector switch**

A 12 point selector switch(TM: OMEGA, Made in USA) has been used in the experiment to measure the temperature of different points on the thermosyphons.

## **3.2 WORKING FLUIDS**

The working fluids used in this study are Methanol ( $\text{CH}_3\text{OH}$ ), Ethanol ( $\text{C}_2\text{H}_5\text{OH}$ ), Acetone ( $\text{CH}_3\text{COCH}_3$ ) and Water ( $\text{H}_2\text{O}$ ). Some important properties of these four working fluids are mentioned below.

**Methanol:** Methanol or Methyl alcohol is a colorless, flame-able liquid. Pure methanol boils at 327.85 K at atmospheric pressure and molecular weight is 32.00. Thermophysical properties of methanol are given in Table-2.

**Ethanol:** Ethanol or Ethyl alcohol is a colorless, flame-able liquid. It boils at 351.3 K at atmospheric pressure. Important properties of ethanol are given in Table-2.

**Acetone:** Acetone is a flame-able, colorless liquid. It is the simplest of the organic chemical called ketones. It is completely soluble in water. It has a mild pleasant odor. It boils at 329 K at atmospheric pressure. Important properties of Acetone are given in Table -2.

**Water :** Water is a colorless liquid. It boils at 373 K at atmospheric pressure. Important properties of Water are given in Table -2.

Table 2 : Thermophysical properties of working fluids

Name of Working Fluid	Density of liquid at $T_{sat}$ , $\rho_l$ (Kg/m <sup>3</sup> )	Density of vapor at $T_{sat}$ , $\rho_v$ (Kg/m <sup>3</sup> )	Boiling Point $T_{sat}$ , °K	Specific heat of liquid at $T_{sat}$ , $C_{p_l}$ (KJ/Kg.K)	Specific heat of vapor at $T_{sat}$ , $C_{p_v}$ (KJ/Kg.K)	Latent heat of vaporization at $T_{sat}$ , $h_{fg}$ (KJ/Kg)	Liquid viscosity, $\mu_l$ ( $\mu$ Ns/m <sup>2</sup> )	Vapor viscosity, $\mu_v$ ( $\mu$ Ns/m <sup>2</sup> )	Prandtl number of liquid ( $Pr_l$ )	Surface tension of vapor liquid interface, $\sigma$ (mN/m)
Acetone (CH <sub>3</sub> COCH <sub>3</sub> )	750.0	2.23	329.25	2.28	1.41	506.0	235.0	9.4	3.77	18.40
Ethanol (C <sub>2</sub> H <sub>5</sub> OH)	757.0	1.435	351.30	3.00	1.83	963.0	428.7	10.4	8.37	17.7
Methanol (CH <sub>3</sub> OH)	751.0	1.222	337.50	2.88	1.55	1101.0	326.0	11.1	5.13	18.75
Water(H <sub>2</sub> O)	958.3	0.597	373.15	4.22	2.03	2256.7	277.53	12.55	1.72	58.91



### 3.3 EXPERIMENTAL PROCEDURE

The Ni-Cr thermic wires are wound around the wall of the evaporator at a constant interval of 1.5 mm. The heat added to the two evaporator sections of MLPT is processed in the electrical method by using the two separate DC power supply. The evaporator sections are covered with glass fiber to minimize heat loss. The adiabatic and the condenser sections are also covered with the insulator.

The condenser sections are cooled by a constant temperature water coolant, circulating in an annular space between the copper tube and jacket. The water coolant is supplied from an elevated water tank and the flow is controlled by the flow meters. Eight calibrated thermocouples of T type are attached at each side at the wall of the MLPT to measure the wall temperature. Four units in the each evaporator section, two units at the each adiabatic section, and two units are at the each condenser section. The inlet and outlet coolant temperatures are also measured. The thermocouples are attached at the wall surface using adhesive. Temperatures are measured by the digital thermometers.

The input power to the heater in the each evaporator section is increased stepwise. The measurements are made under a steady state condition at each input power. Ethanol, methanol, acetone and water are used as the working fluid. To understand the effects the coolant flow rate and heat flux are changed.

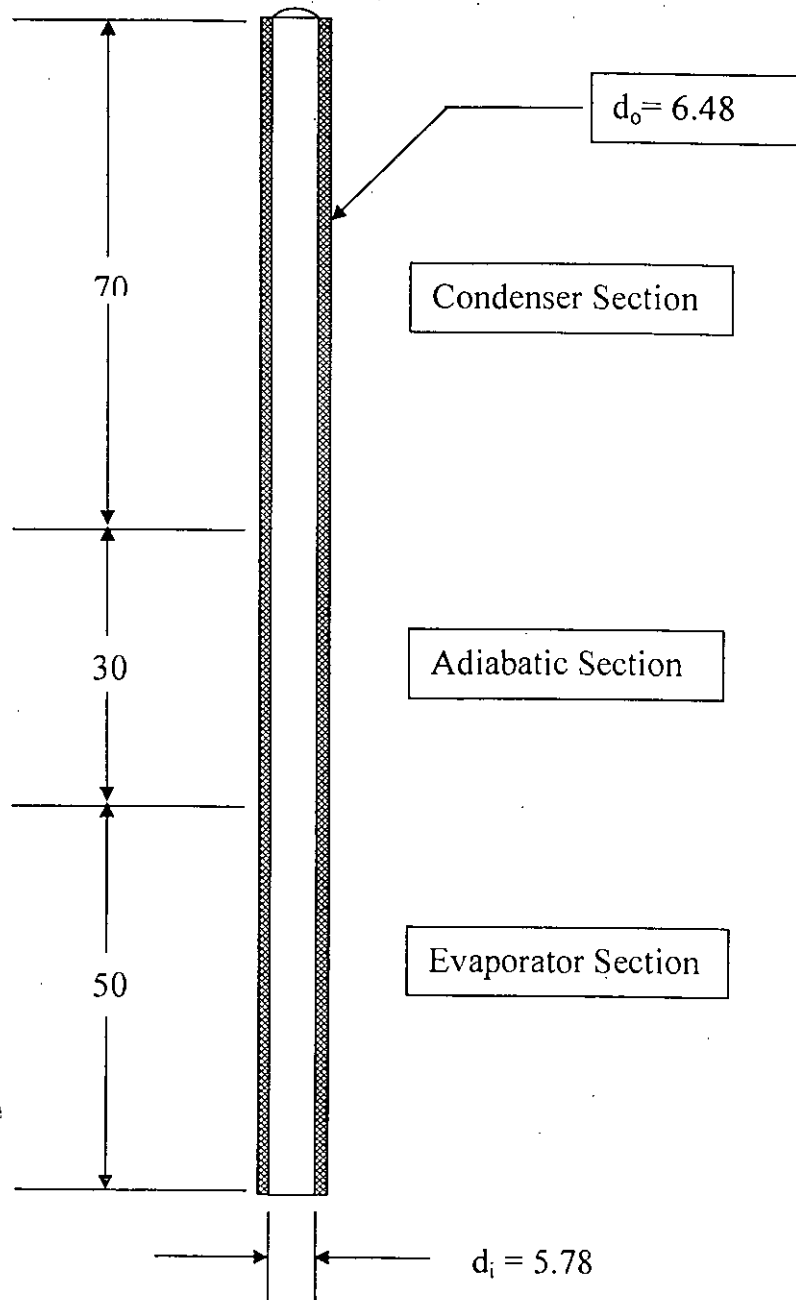
### 3.4 MATHEMATICAL EQUATION

In the present study, the performance of LPT is evaluated by measuring the thermal resistance,  $R$  ( $^{\circ}\text{C}/\text{W}$ ), which is defined in Equation (1)

$$R = \frac{T_e - T_c}{Q} \quad (1)$$

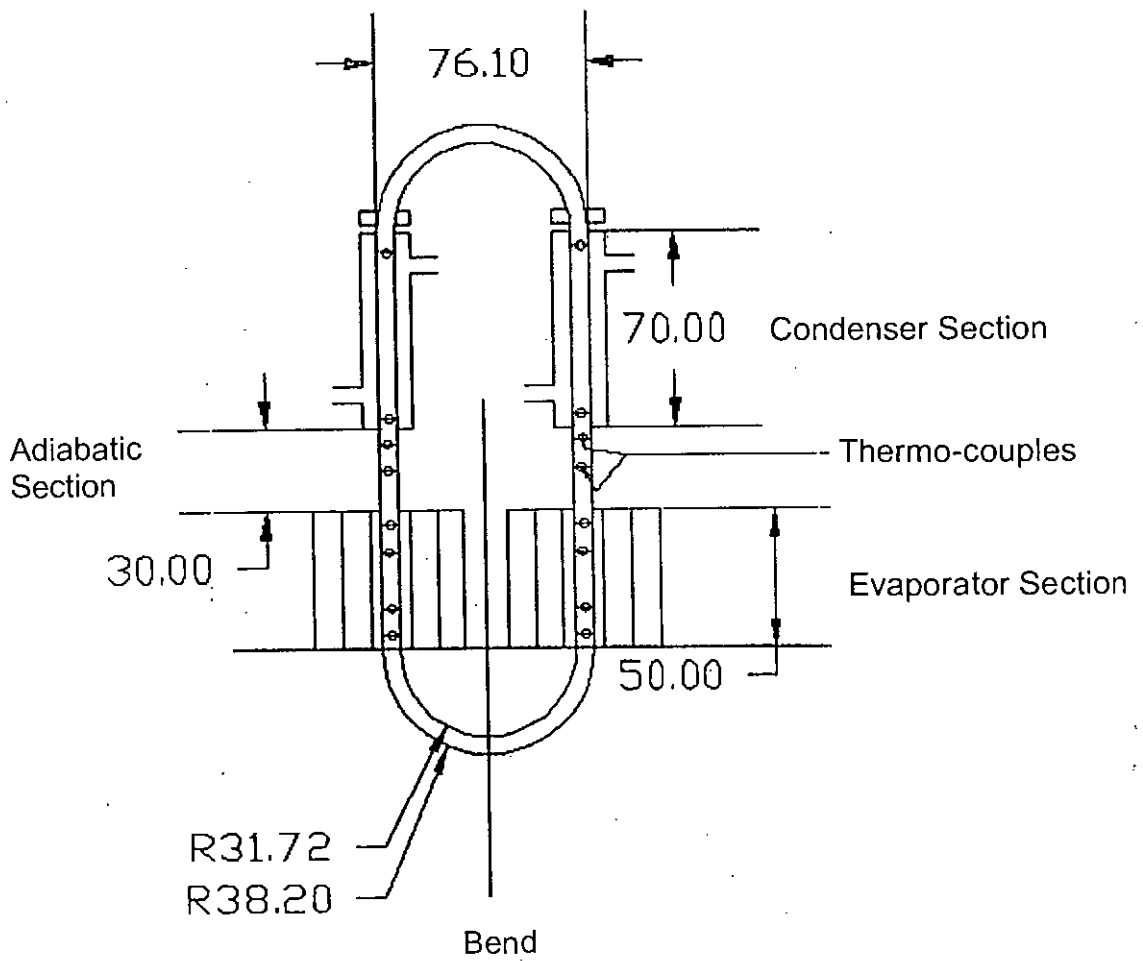
The overall heat transfer coefficient,  $U_t$  ( $\text{kW}/\text{m}^2\text{ }^{\circ}\text{C}$ ) is obtained from Equation (2) as follows

$$U_t = \frac{Q}{A_e(T_e - T_c)} \quad (2)$$



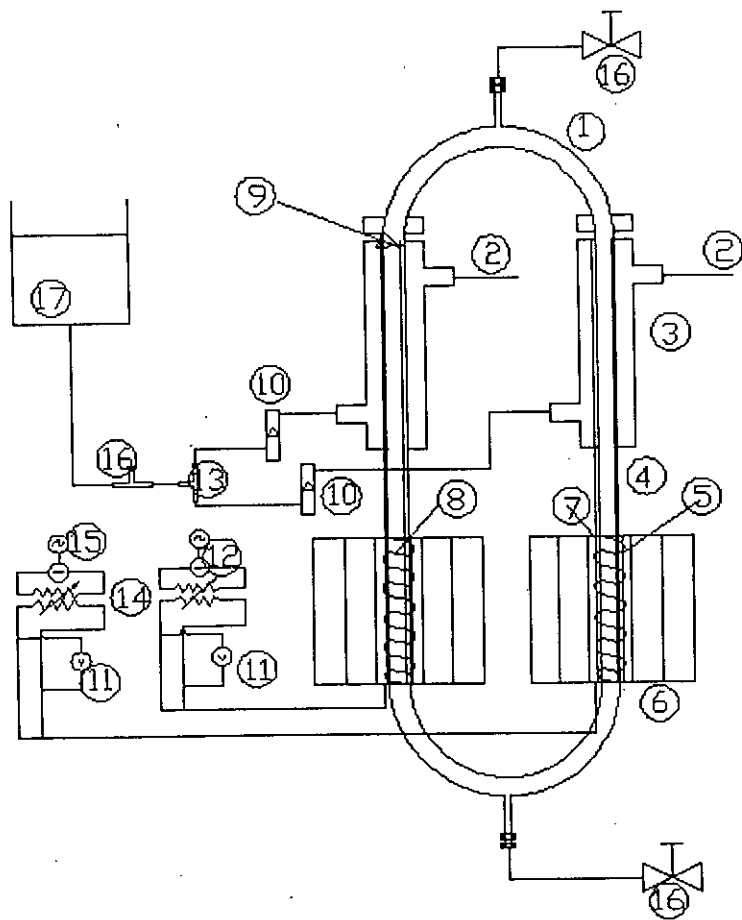
(All dimensions are in mm)

Figure. 3.1.a dimensions of thermosyphon



(All dimensions are in mm)

Fig.3.1.b Schematic diagram of the looped parallel thermosyphon



1. U-Tube
2. Water out
3. Condenser
4. Adiabatic section
5. Evaporator section
6. Insulator
7. Mica sheet
8. Heater
9. Insulating tape
10. Flow meter
11. Volt meter
12. D.C. power source
13. T-joint
14. Volt slider
15. A.C. power source
16. Gate valve
17. Water tank

Fig.3.1.c Experimental apparatus

---

## RESULTS AND DISCUSSION

For better understanding the heat transfer characteristics of thermosyphon the wall temperature at different points of the two phase looped thermosyphon are measured. From these measured data the temperature profiles are plotted against the axial distances. By using the equation (1) and (2) thermal resistance,  $R$  and overall heat transfer coefficient,  $U_t$  is determined. Each of these properties are compared and explained in detail on the following section with graphs.

### 4.1 Temperature profile along the wall of the two phase looped thermosyphon

Figures 4.1.1-1(a) to (f) show the wall temperature profiles along the axial length from the bottom of the thermosyphon having 5.78 mm ID at various heat flux for acetone. Figures indicate that temperature of the evaporator sections increases with increasing heat flux at all coolant flow rate conditions. At a particular heat flux condition, the temperatures of the both sides of the evaporator sections gradually decrease along the height. Again the temperature of the evaporator sections decreases with the increase in coolant flow rate within the experimental range. At higher coolant flow rate of 1.0 l/min and higher heat flux condition of  $7.35 \text{ kW/m}^2$ , the average temperature of left hand side of the evaporator sections is found to be  $84.3 \text{ }^\circ\text{C}$  shown in shown in Fig.4.1.1-1(e). At the same conditions, the average temperature of right hand side of the evaporator section is found to be  $85.3 \text{ }^\circ\text{C}$  shown in shown in Fig.4.1.1-1(f). Therefore, no significant variation in temperature between the left hand and right hand sides of MLPT is observed.

Figures 4.1.1-2(a) to (f) show the wall temperature profiles along the axial length from the bottom of thermosyphon for ethanol working fluid at various heat flux. Figures indicate the similar result as found for acetone. At higher coolant flow rate of 1 l/min and higher heat flux condition of  $7.35 \text{ kW/m}^2$ , the average temperature of left hand side of the evaporator sections is found to be  $77.3 \text{ }^\circ\text{C}$  as shown in Fig.4.1.1-2(e). At same conditions, the average temperature of right hand side of the evaporator sections is found to be  $78.5 \text{ }^\circ\text{C}$  as shown in Fig.4.1.1-2(f). Therefore, at the same experimental conditions the average wall temperature of the evaporator sections for ethanol is found to be about  $7^\circ\text{C}$  lower than that for acetone.

Figures 4.1.1-3(a) to (f) show the wall temperature profiles along the axial length from the bottom of thermosyphon for methanol working fluid at various heat flux. Figures indicate the similar result as found for acetone. At higher coolant flow rate of 1 l/min and higher heat flux condition of  $7.35 \text{ kW/m}^2$ , the average temperature of left hand side of the evaporator sections is found to be  $84^\circ\text{C}$  as shown in Fig.4.1.1-3(e). At same conditions, the average temperature of right hand side of the evaporator sections is found to be  $85^\circ\text{C}$  as shown in Fig.4.1.1-3(f). Therefore; at the same experimental conditions the average wall temperatures of the evaporator sections are found almost same values for both methanol and acetone.

Figures 4.1.1-4(a) to (f) show the wall temperature profiles along the axial length from the bottom of thermosyphon for water working fluid at various heat flux. Figures indicate the similar result as found for acetone. At higher coolant flow rate of 1 l/min and higher heat flux condition of  $7.35 \text{ kW/m}^2$ , the average temperature of left hand side of the evaporator sections is found to be  $87.2^\circ\text{C}$  as shown in Fig.4.1.1-4(e). At same conditions, the average temperature of right hand side of the evaporator sections is found to be  $88.4^\circ\text{C}$  as shown in Fig.4.1.1-4(f). At the same experimental conditions the average wall temperatures of the evaporator sections for water are found to be maximum than those for acetone, ethanol and methanol.

Figures 4.1.2-1 (a) to (d) show the axial wall temperature distributions of the MLPT at various coolant flow rate for acetone working fluid. Figures indicate that both the condenser and evaporator wall temperatures decreases with the increase in coolant flow rate. At the higher heat flux condition of  $7.35 \text{ kW/m}^2$  and lower coolant flow rate of 0 l/min, the average temperature of left hand side of the evaporator sections is found to be  $109^\circ\text{C}$ . At the same conditions, the average temperature of right hand side of the evaporator sections is found to be  $110^\circ\text{C}$ . At the higher heat flux condition and higher coolant flow rate of 1.0 l/min, the average temperature of the evaporator sections are found to be  $84.3^\circ\text{C}$  and  $85.3^\circ\text{C}$  in the LHS and RHS, respectively. At zero coolant flow rate, the difference in temperature between evaporator and condenser sections is not so large for all heat flux conditions within the experimental range. And the average wall temperature of the evaporator sections is about  $25^\circ\text{C}$  higher than that for higher coolant flow rate of 1.0 l/min.

Figures 4.1.2-2 (a) to (d) show the axial wall temperature distribution of the MLPT at various coolant flow rate for ethanol working fluid. Figures indicate that both the condenser and evaporator wall temperatures decreases with the increase in coolant flow rate. At the higher heat flux condition of  $7.35 \text{ kW/m}^2$  and lower coolant flow rate of 0 l/min, the average temperature of left hand side of the evaporator sections is found to be  $96^\circ\text{C}$ . At the same conditions, the average

temperature of right hand side of the evaporator sections is found to be  $97^{\circ}\text{C}$ . At the higher heat flux condition and higher coolant flow rate of  $1.0\text{ l/min}$ , the average temperature of the evaporator sections are found to be  $77.3^{\circ}\text{C}$  and  $78.5^{\circ}\text{C}$  in the LHS and RHS, respectively. At zero coolant flow rate, the difference in temperature between evaporator and condenser sections is not so large for all heat flux conditions within the experimental range. At zero coolant flow rate, the average wall temperature of the evaporator sections is about  $19^{\circ}\text{C}$  higher than that for higher coolant flow rate of  $1.0\text{ l/min}$ .

Figures 4.1.2-3 (a) to (d) show the axial wall temperature distribution of the MLPT at various coolant flow rate for methanol working fluid. Figures indicate the similar result as found for acetone. At the higher heat flux condition of  $7.35\text{ kW/m}^2$  and lower coolant flow rate of  $0\text{ l/min}$ , the average temperature of left hand side of the evaporator sections is found to be  $108^{\circ}\text{C}$ . At the same conditions, the average temperature of right hand side of the evaporator sections is found to be  $109^{\circ}\text{C}$ . At the higher heat flux condition and higher coolant flow rate of  $1.0\text{ l/min}$ , the average temperature of the evaporator sections are found to be  $84^{\circ}\text{C}$  and  $85^{\circ}\text{C}$  in the LHS and RHS, respectively. At zero coolant flow rate, the difference in temperature between evaporator and condenser sections is not so large for all heat flux conditions within the experimental range. At zero coolant flow rate, the average wall temperature of the evaporator sections is about  $24^{\circ}\text{C}$  higher than that for higher coolant flow rate of  $1.0\text{ l/min}$ .

Figures 4.1.2-4 (a) to (d) show the axial wall temperatures distribution of the MLPT at various coolant flow rate for water working fluid. At the higher heat flux condition of  $7.35\text{ kW/m}^2$  and lower coolant flow rate of  $0\text{ l/min}$ , the average temperature of left hand side of the evaporator sections is found to be  $111^{\circ}\text{C}$ . At the same conditions, the average temperature of right hand side of the evaporator sections is found to be  $112^{\circ}\text{C}$ . At the higher heat flux condition and higher coolant flow rate of  $1.0\text{ l/min}$ , the average temperature of the evaporator sections are found to be  $87.8^{\circ}\text{C}$  and  $89^{\circ}\text{C}$  in the LHS and RHS, respectively. At zero coolant flow rate, the difference in temperature between evaporator and condenser sections is not so large for all heat flux conditions within the experimental range. At zero coolant flow rate, the average wall temperature of the evaporator sections is about  $23^{\circ}\text{C}$  higher than that for higher coolant flow rate of  $1.0\text{ l/min}$ .

#### **4.2 (a) Effect of coolant flow rate on thermal resistance:**

Figures 4.2.1(a) to (h) show the change in the thermal resistance according to the coolant flow rate in the condenser within the stable operational zone where no dryout occurs for all working

fluids. For acetone the thermal resistance is found to be minimum at all heat flux conditions at zero coolant flow rate and increases up to a low coolant flow rate of 0.12 l/min as shown in (a) and (b). Beyond this value the thermal resistance is almost independent of coolant flow rate. For ethanol shown in (c) and (d) indicates similar trends up to a low coolant flow rate of 0.12 l/min. But beyond this value the thermal resistance gradually decreases with increase in coolant flow rate. Results for methanol and water shown in (e) and (f), and (g) and (h), respectively indicate almost similar trends of ethanol.

#### **4.2(b) Effect of heat flux on thermal resistance:**

Figures 4.2.2(a) to (h) show the thermal resistance of thermosyphon as a function of thermal load. The thermal resistance exhibited a decreasing trend as the thermal load is increased except at zero coolant flow rate for all working fluids. It is suspected that as the thermal load is raised, heat transfer rate is increased due to the increase of vapor density.

#### **4.2(c) Effect of working fluids on thermal resistance:**

Effects of working fluids on the thermal resistance are shown in Fig. 4.3.1 (a) and (b). At higher heat flux condition, the thermal resistance of MLPT increases with increase in coolant flow rate up to 0.12 l/min. But beyond this value the thermal resistance gradually decreases with increase in coolant flow rate for all working fluids as shown in Fig. 4.3.1 (a). Thermal resistances of MLPT are found to 3.05 °C/W, 2.89 °C/W, 3.01 °C/W and 3.92 °C/W for acetone, ethanol, methanol and water respectively. At higher coolant flow rate of 1.0 l/min, the thermal resistance of MLPT gradually decreases with increase in heat flux for all working fluids as shown in Fig. 4.3.1 (b).

#### **4.3(d) Effect of working fluids on overall heat transfer coefficient:**

Effects of working fluids on the overall heat transfer coefficient are shown in Fig. 4.3.2 (a) and (b). At higher heat flux condition, the overall heat transfer coefficients of MLPT decrease with increase in coolant flow rate up to 0.12 l/min. But beyond this value the heat transfer coefficient gradually increases with increase in coolant flow rate for all working fluids as shown in Fig. 4.3.1 (a). The overall heat transfer coefficients of MLPT are found to 0.160 kW/m<sup>2</sup>°C, 0.169 kW/m<sup>2</sup>°C, 0.162 kW/m<sup>2</sup>°C and 0.125 kW/m<sup>2</sup>°C for acetone, ethanol, methanol and water respectively. At higher coolant flow rate of 1.0 l/min the overall heat transfer coefficients of MLPT gradually increases with increase in heat flux for all working fluids as shown in Fig. 4.3.2(b). The overall heat transfer coefficient of MLPT for ethanol shows the highest value of 0.169kW/m<sup>2</sup>°C and for water shows the lowest value of 0.125 kW/m<sup>2</sup>°C.



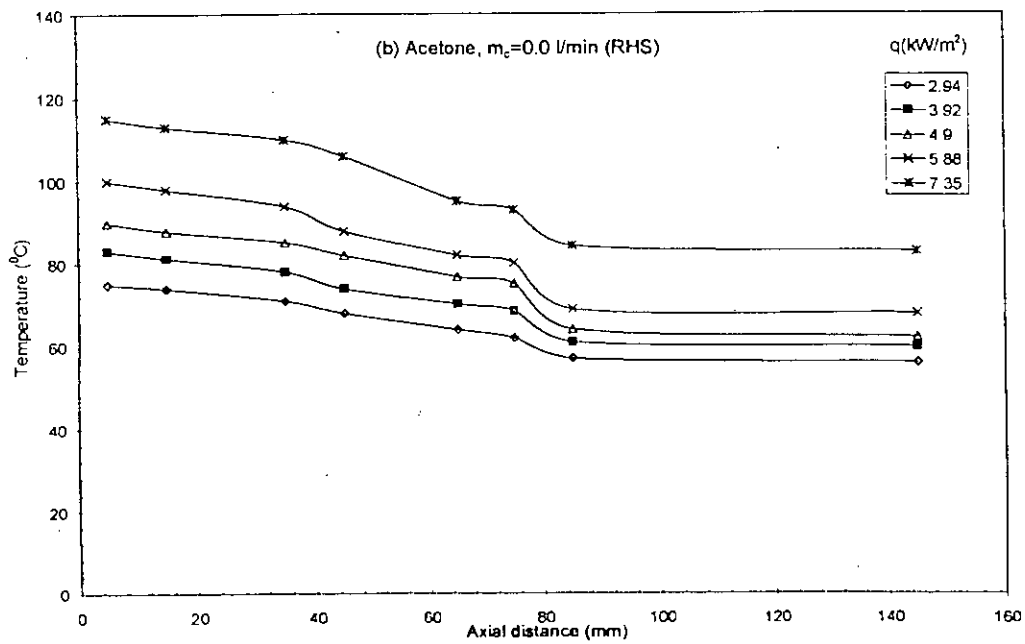
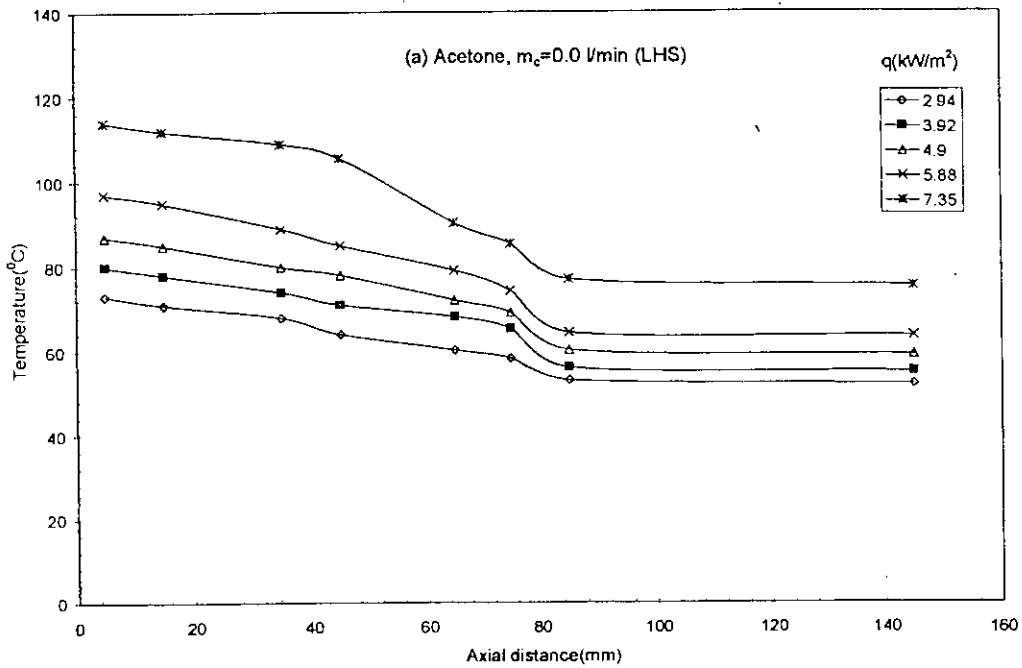


Figure 4.1.1-1 Temperature distribution for various heat flux

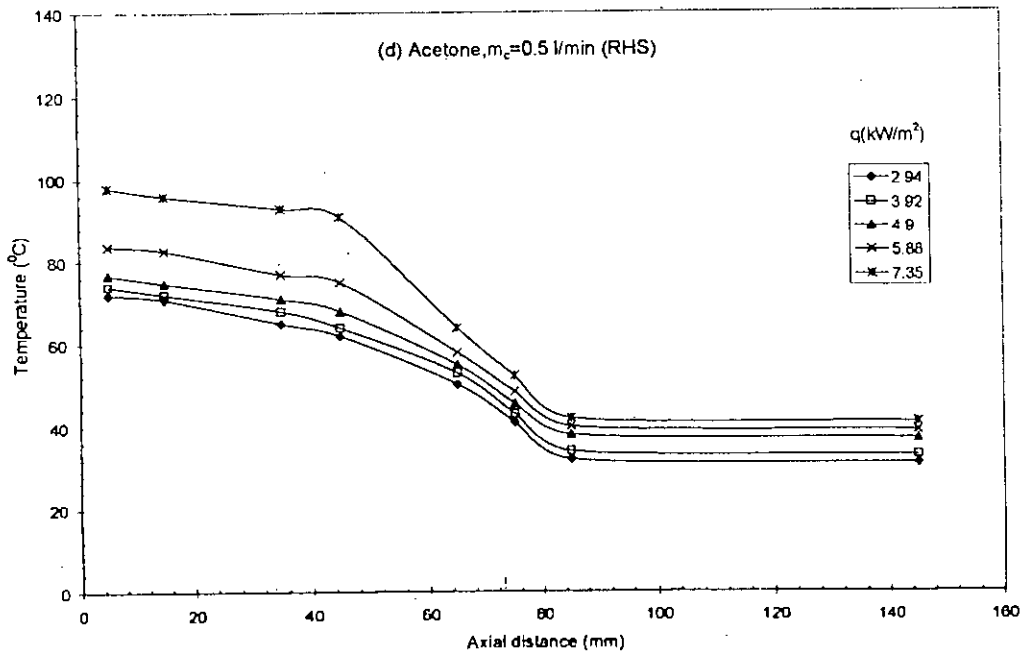
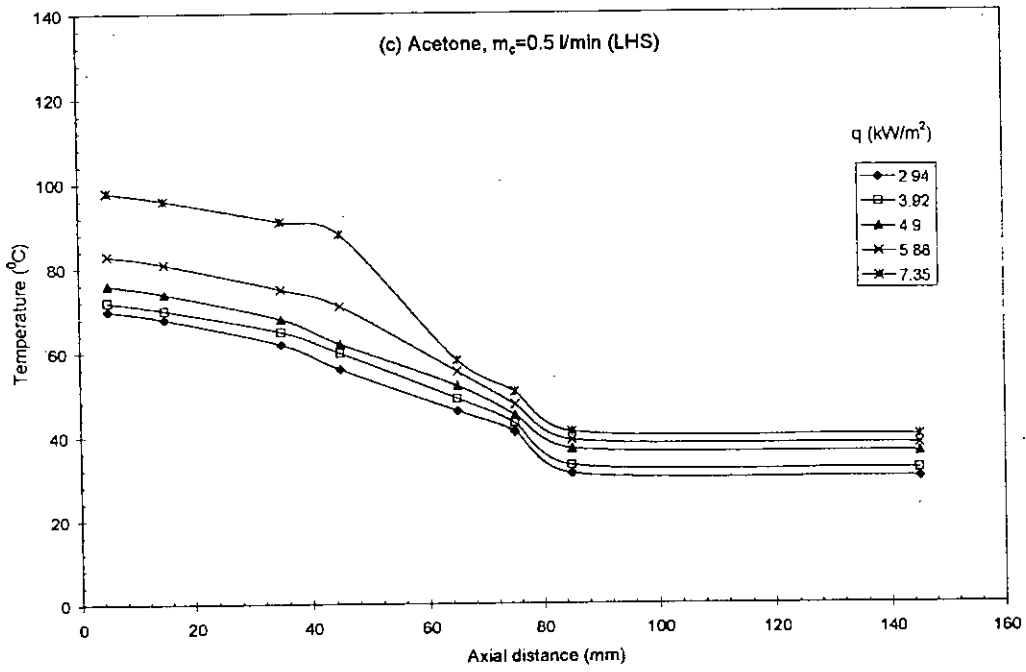


Figure 4.1.1-1 Temperature distribution for various heat flux

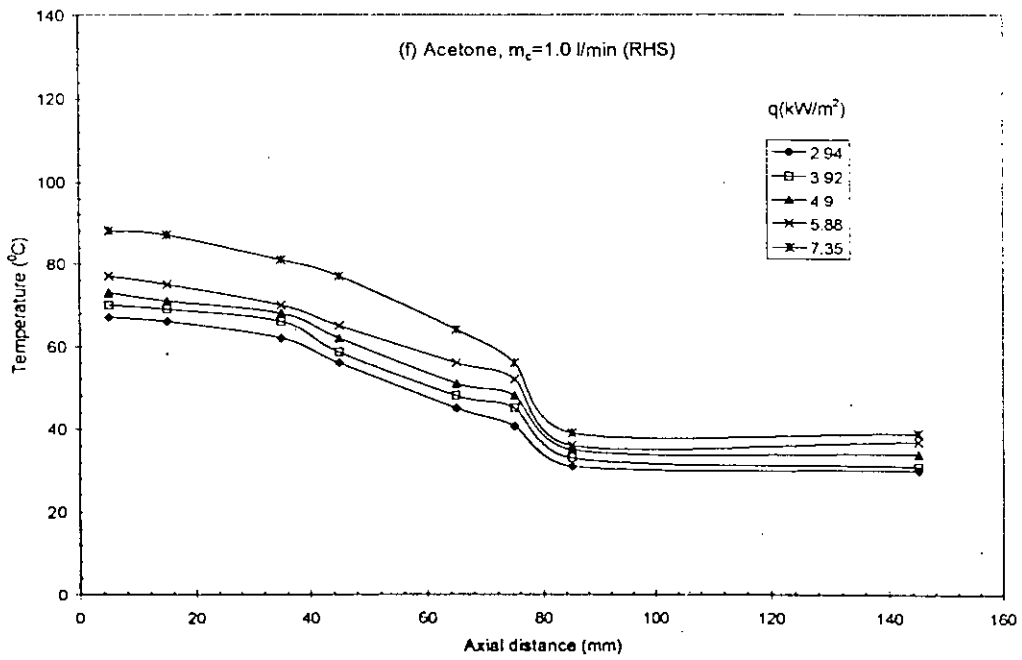
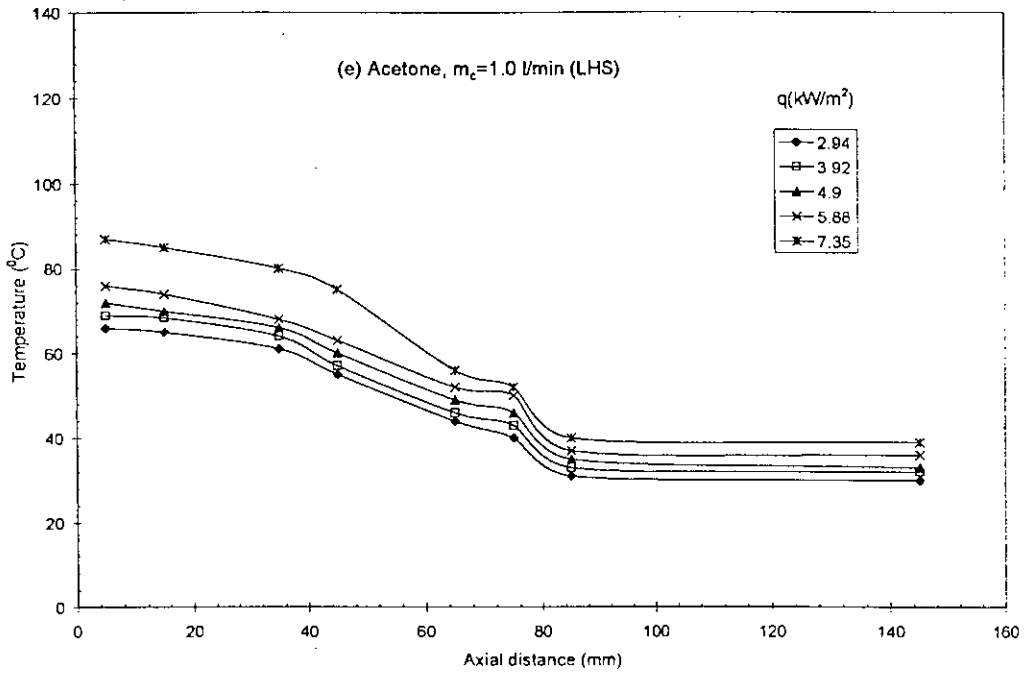


Figure 4.1.1-1 Temperature distribution for various heat flux

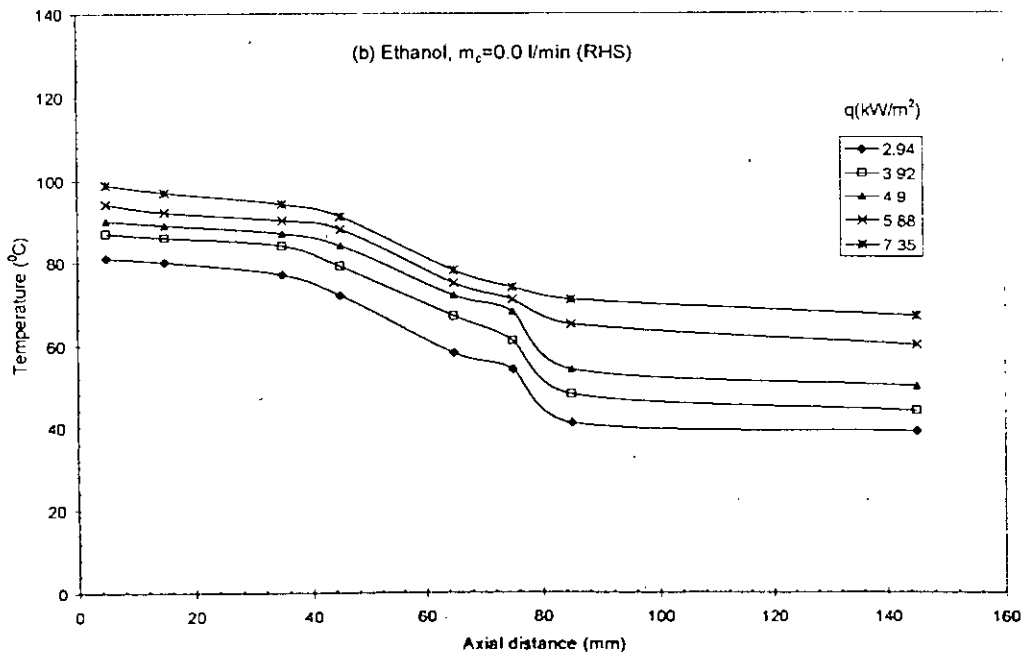
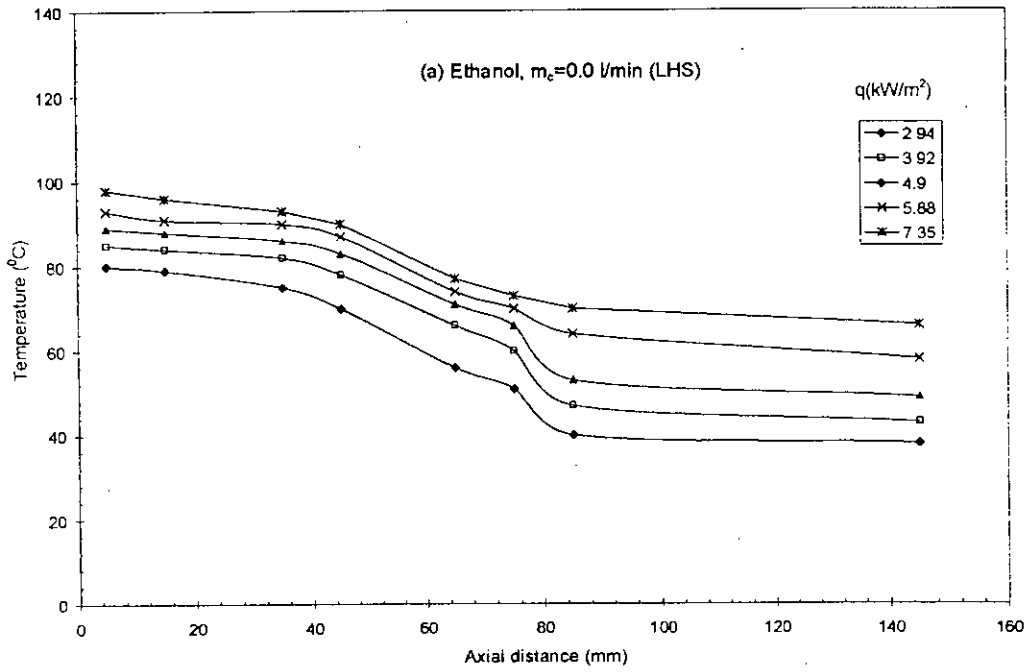


Figure 4.1.1-2 Temperature distribution for various heat flux

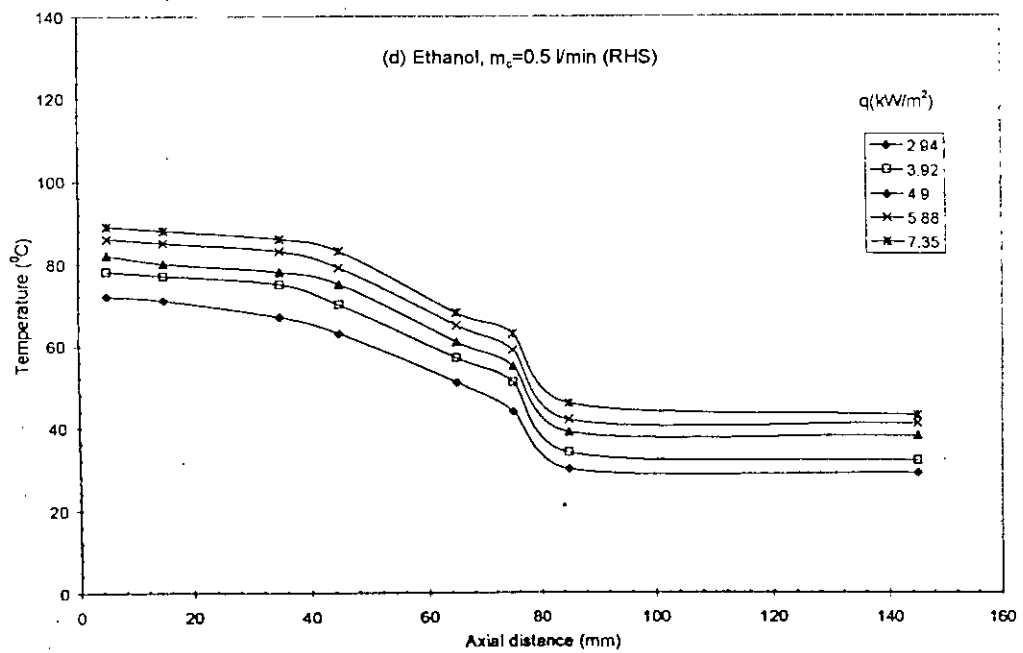
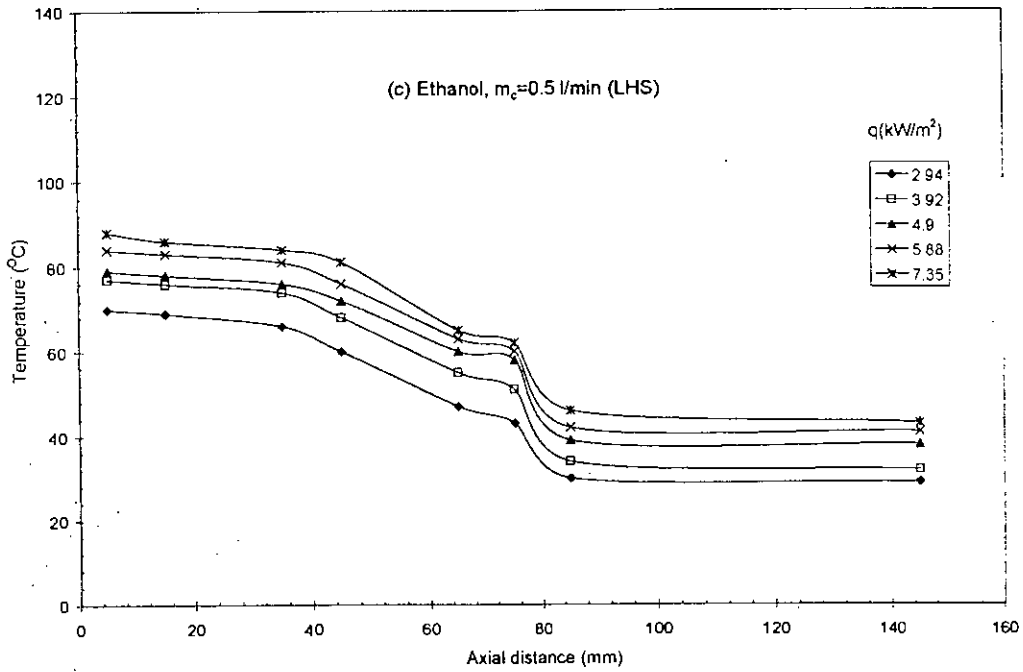


Figure 4.1.1-2 Temperature distribution for various heat flux

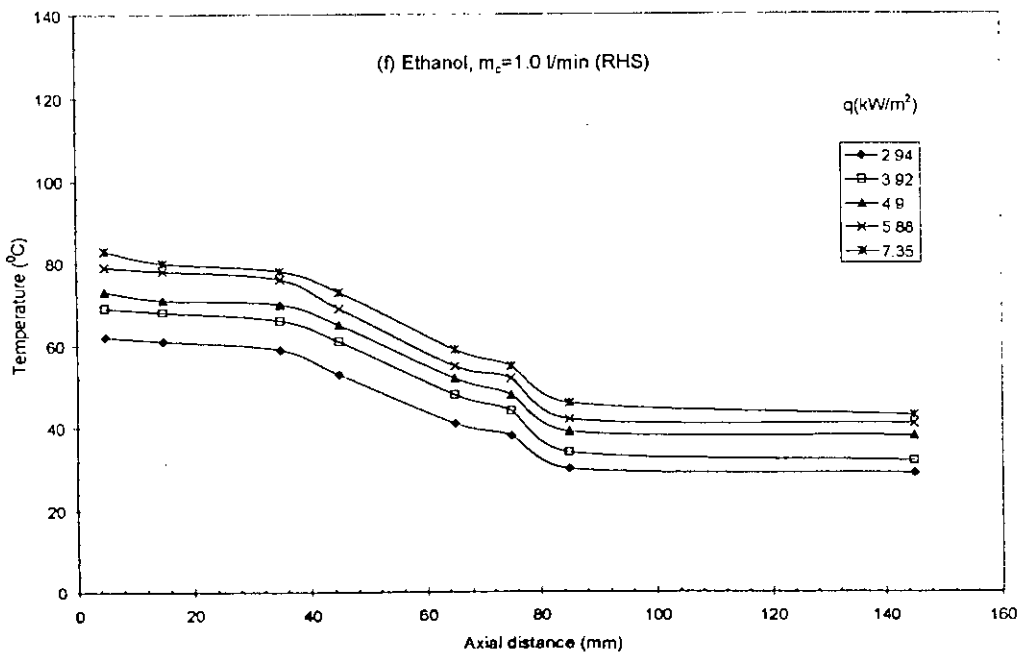
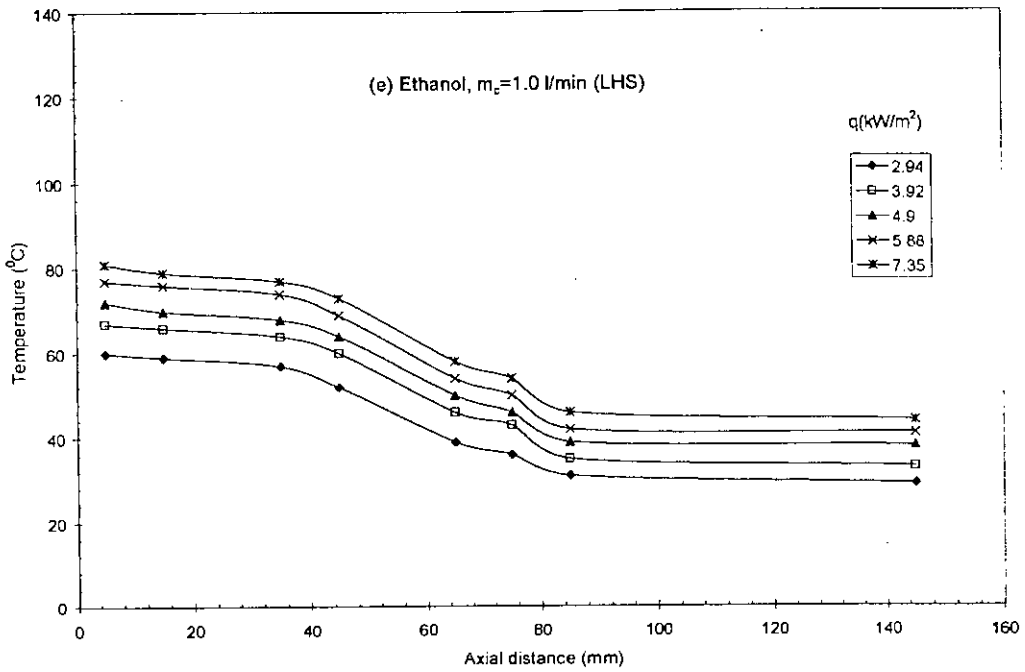


Figure 4.1.1-2 Temperature distribution for various heat flux

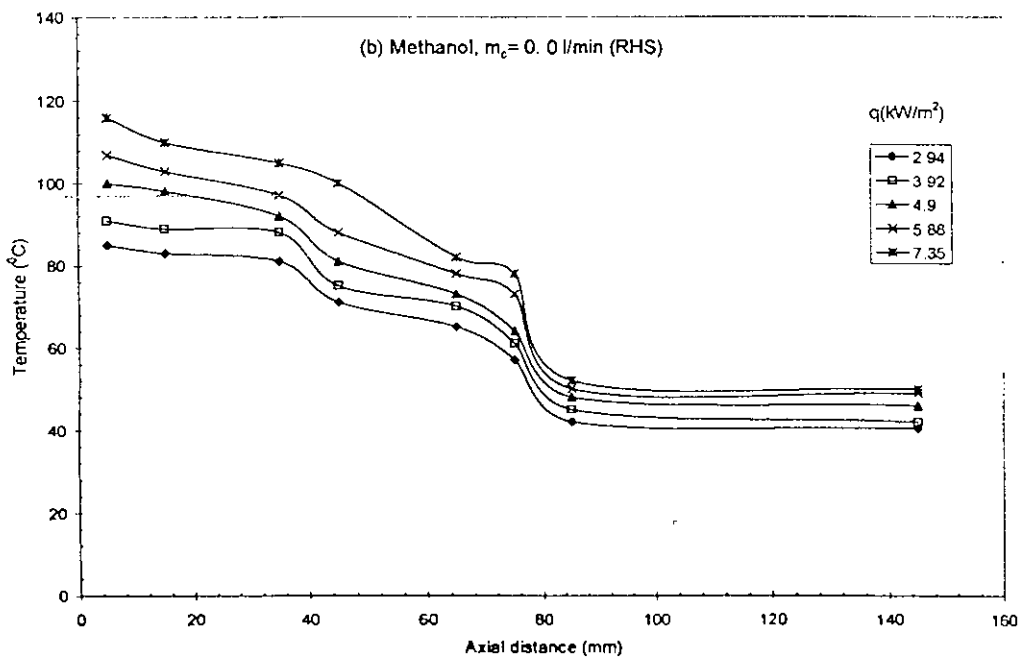
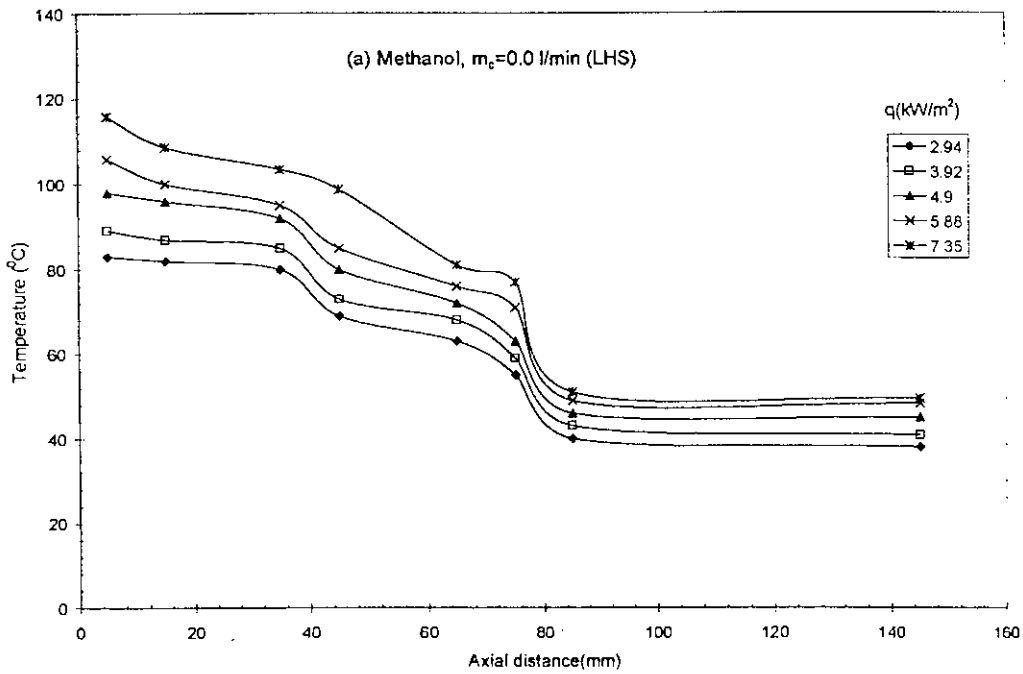


Figure 4.1.1-3 Temperature distribution for various heat flux

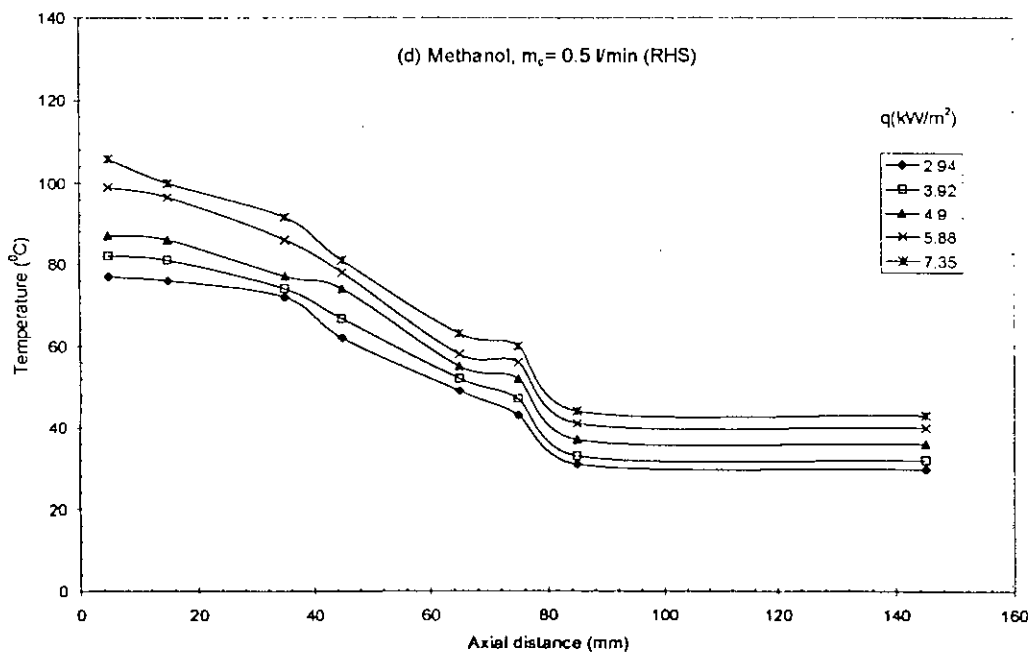
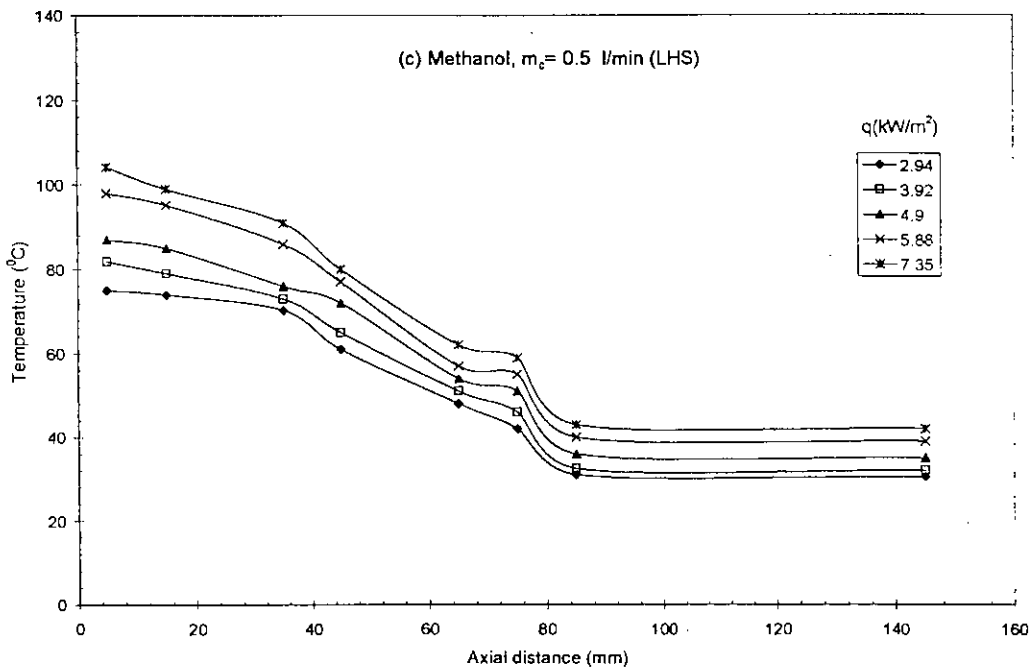


Figure 4.1.1-3 Temperature distribution for various heat flux



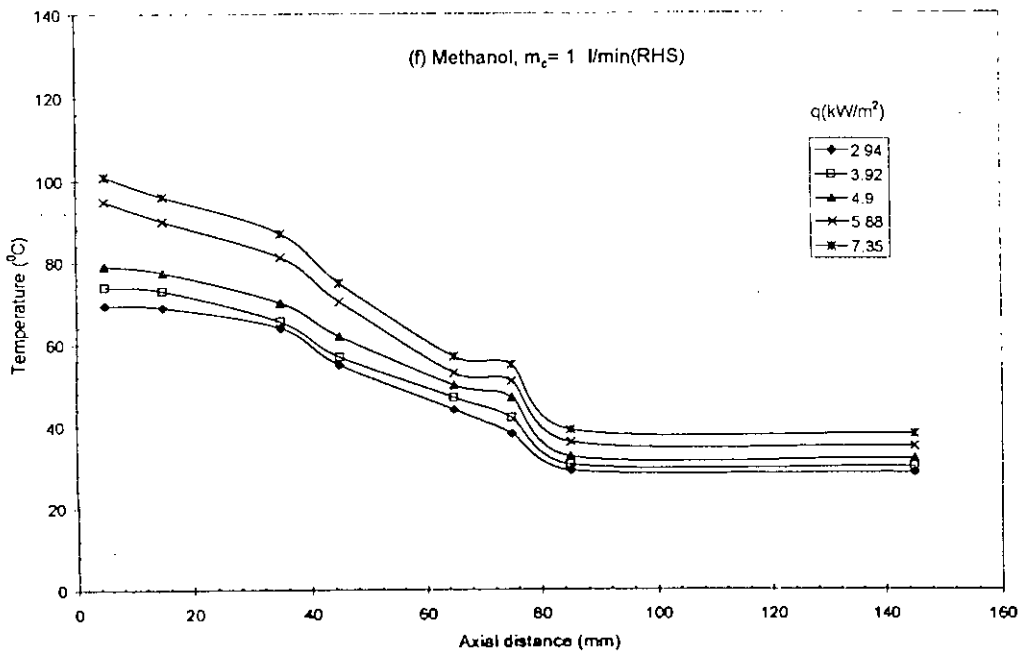
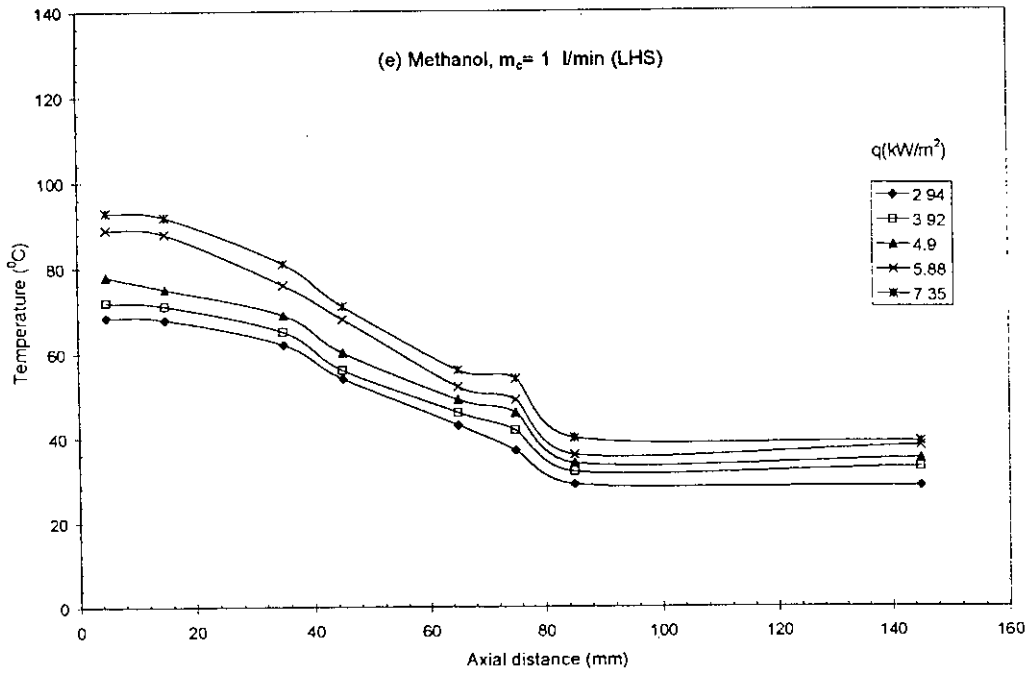


Figure 4.1.1-3 Temperature distribution for various heat flux

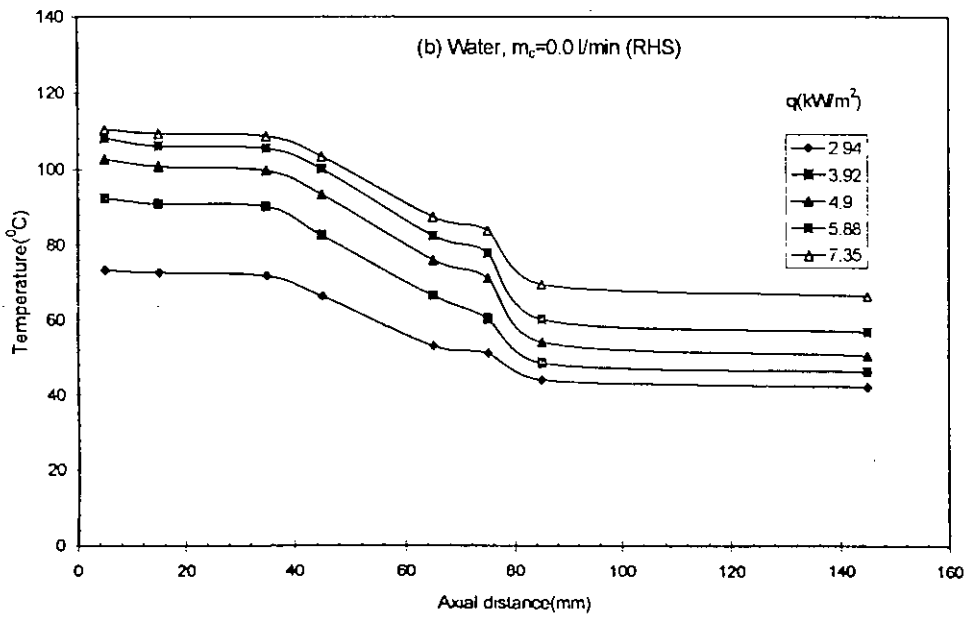
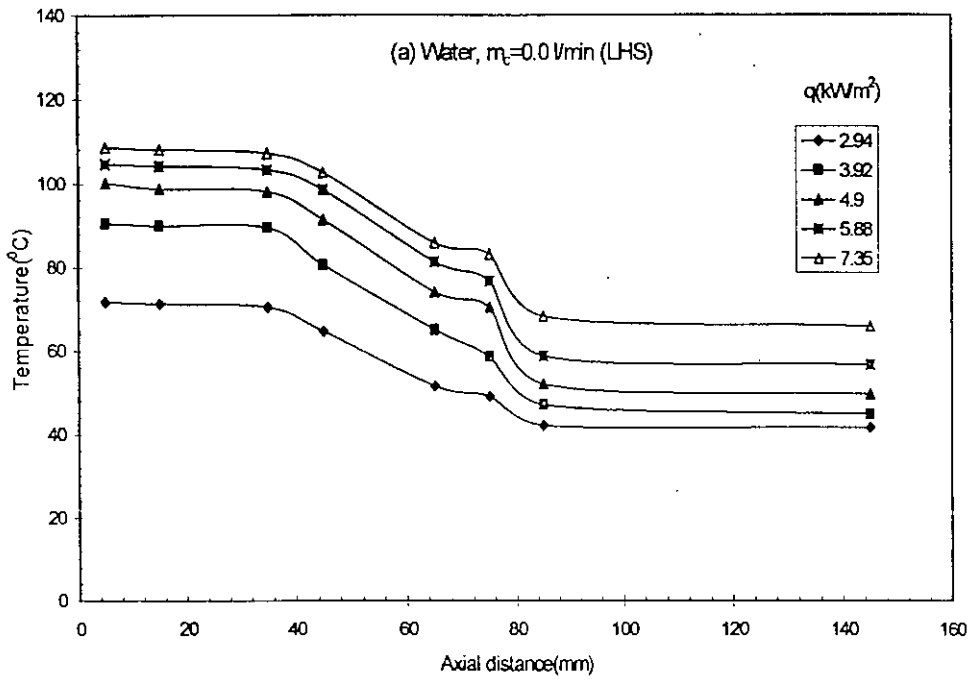


Figure 4.1.1-4 Temperature distribution for various heat flux

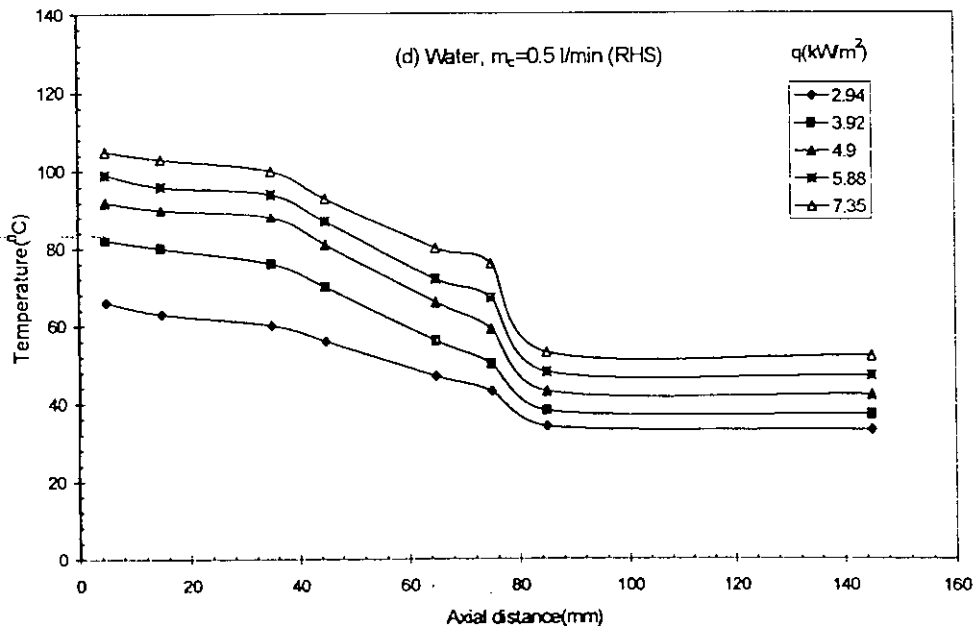
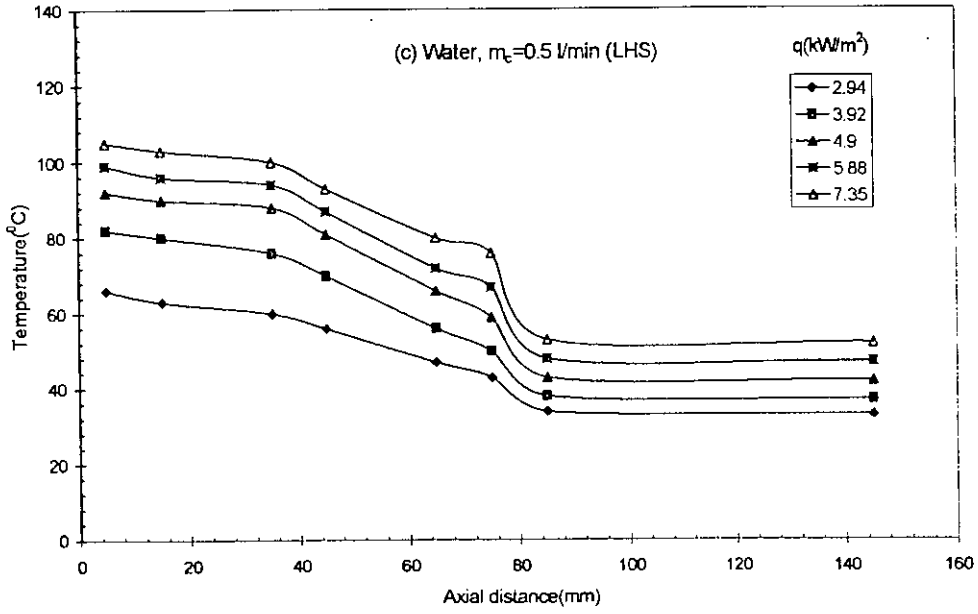


Figure 4.1.1-4 Temperature distribution for various heat flux

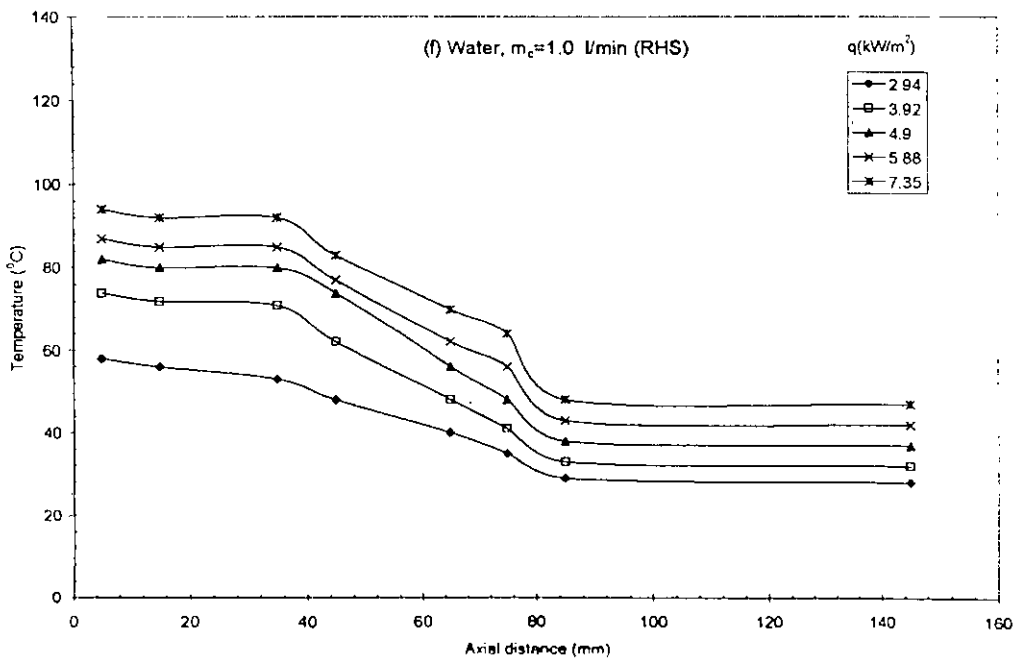
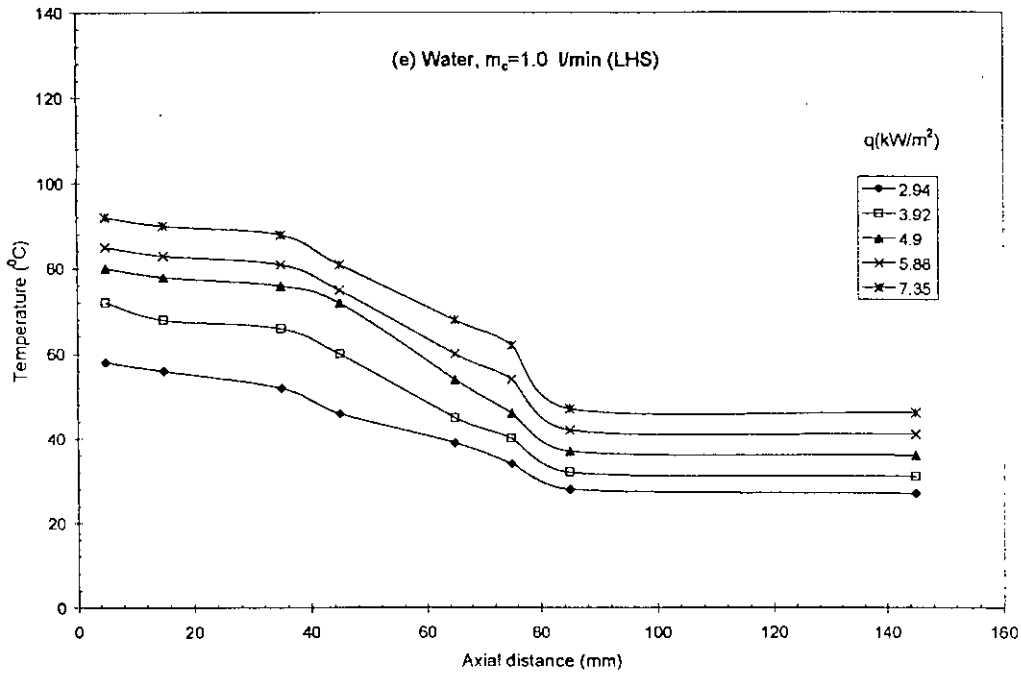


Figure 4.1.1-4 Temperature distribution for various heat flux

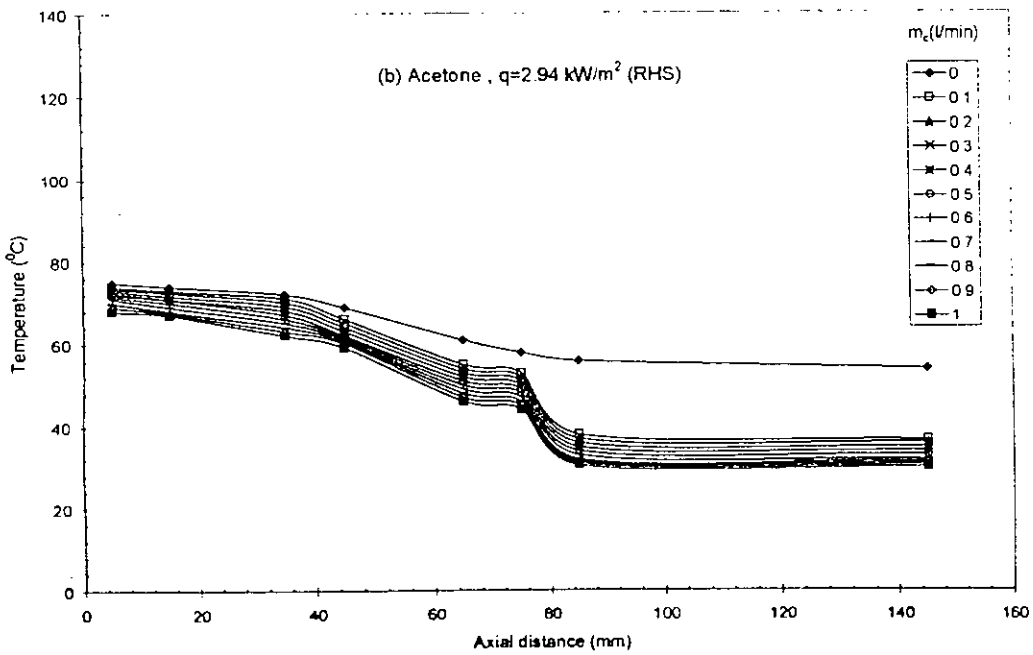
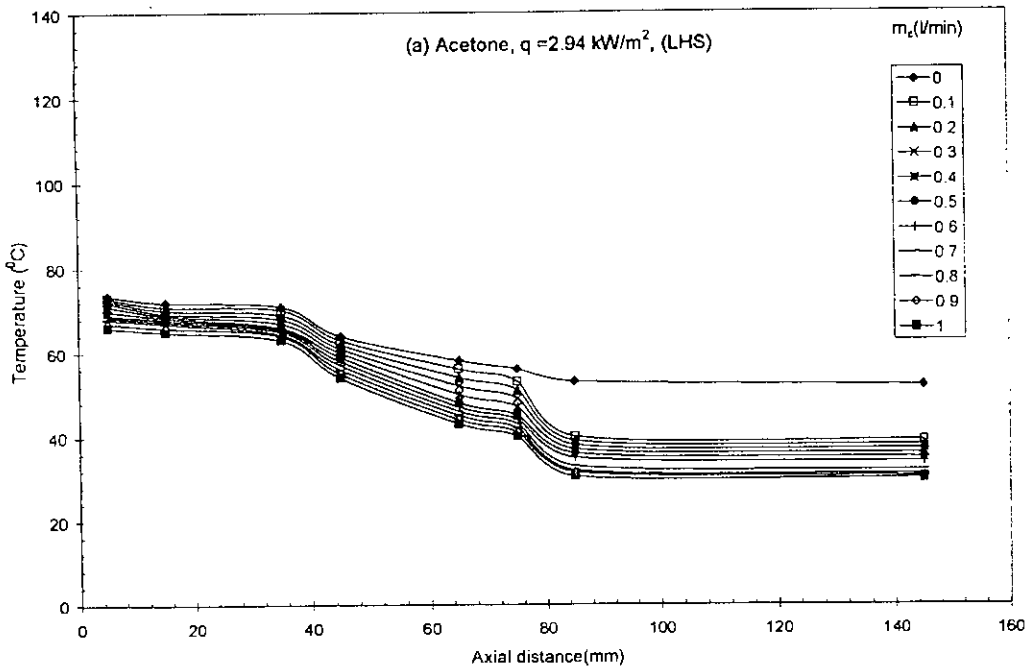


Figure 4.1.2-1 Temperature distribution for various coolant flow rate

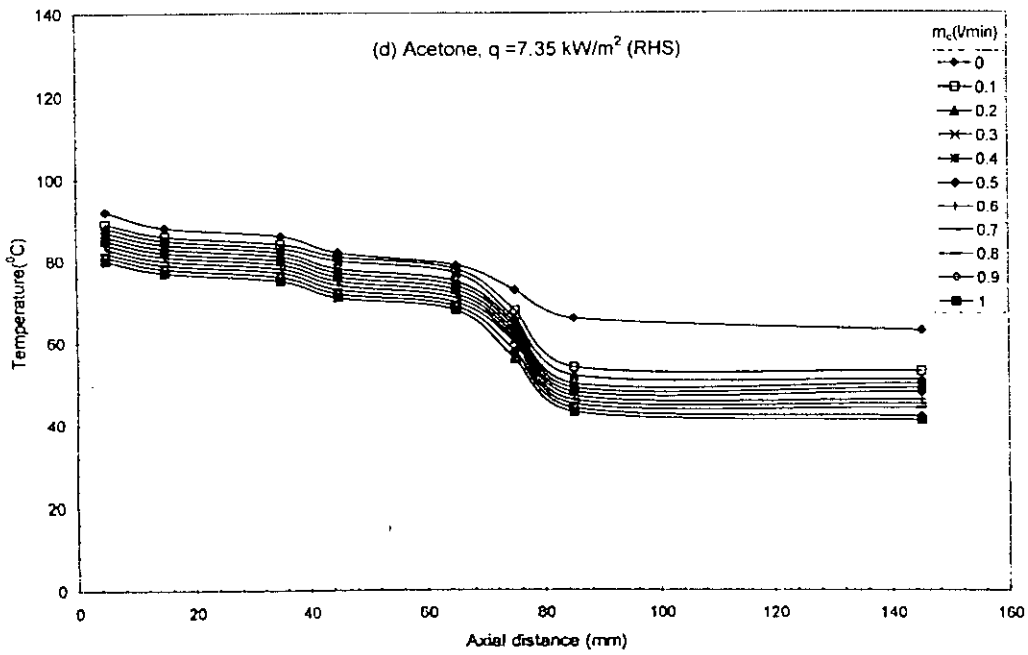
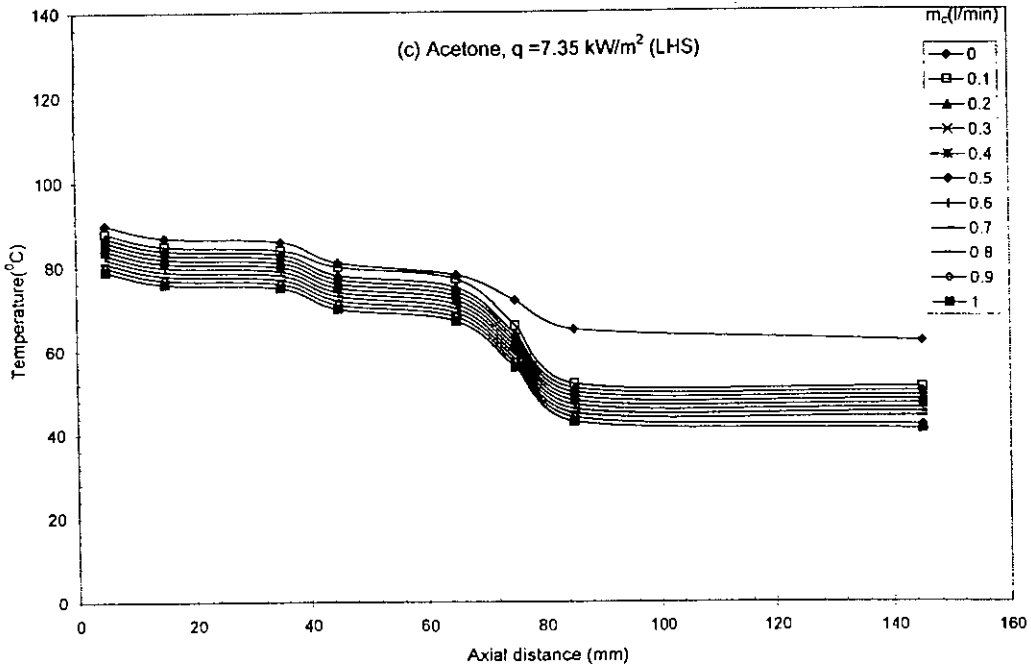


Figure 4.1.2-1 Temperature distribution for various coolant flow rate

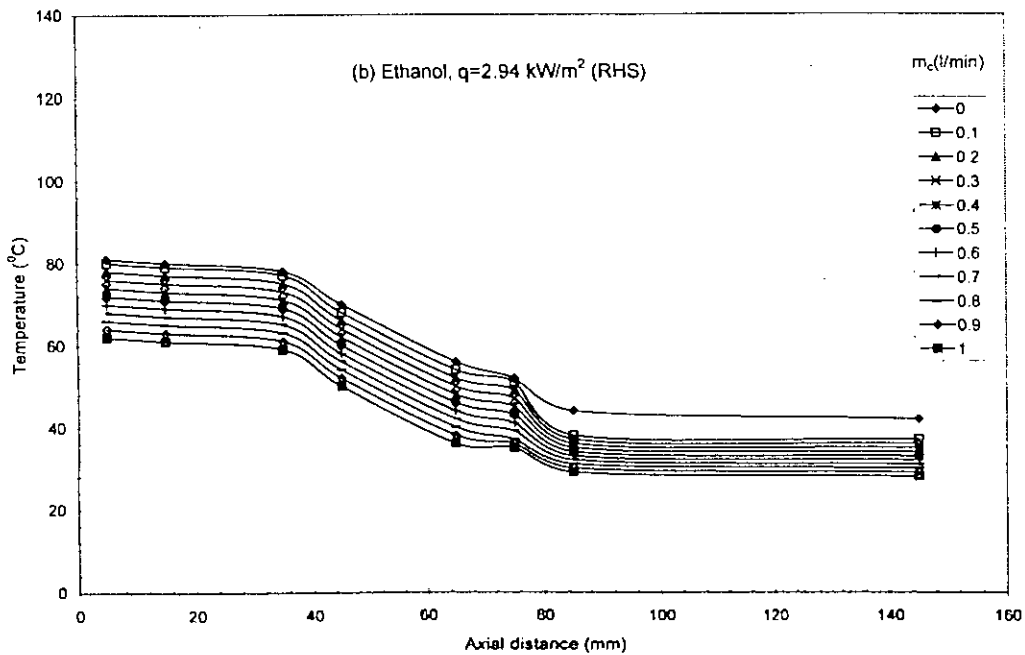
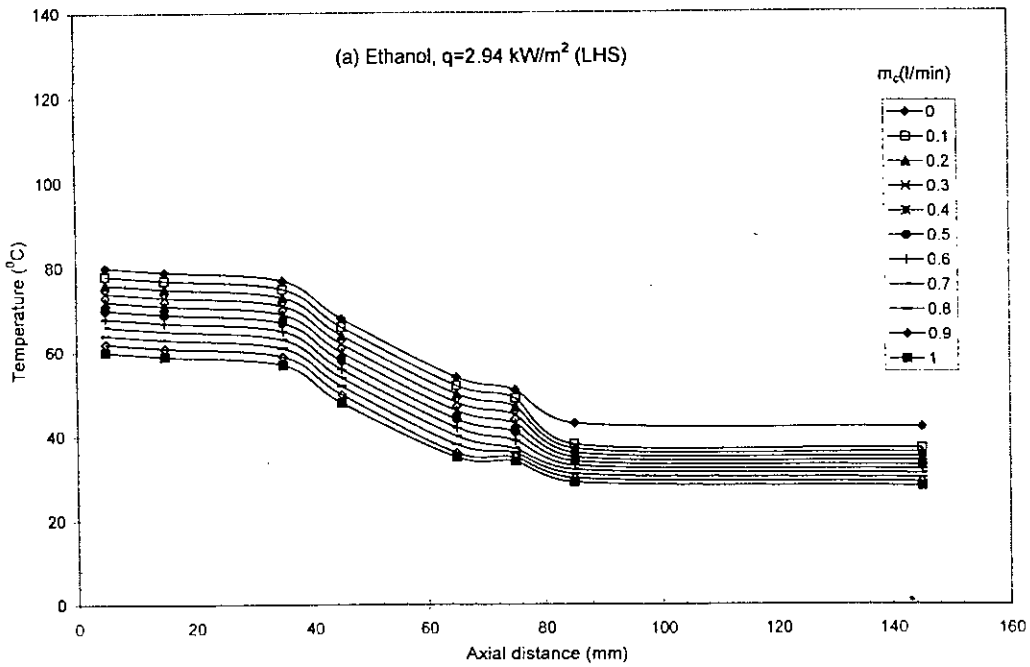


Figure 4.1.2-2 Temperature distribution for various coolant flow rate

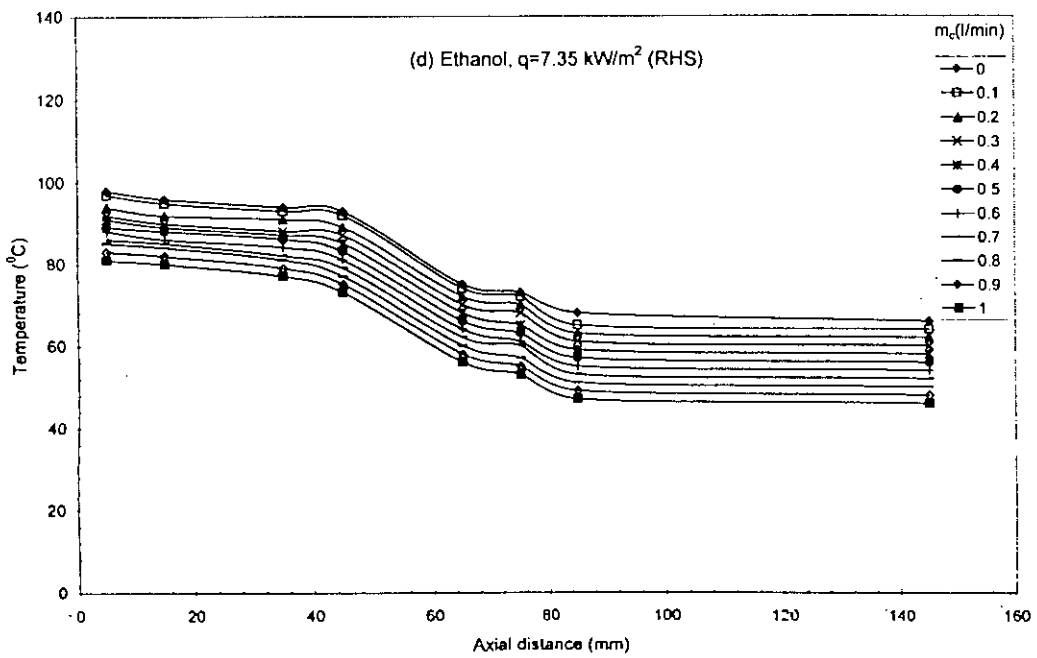
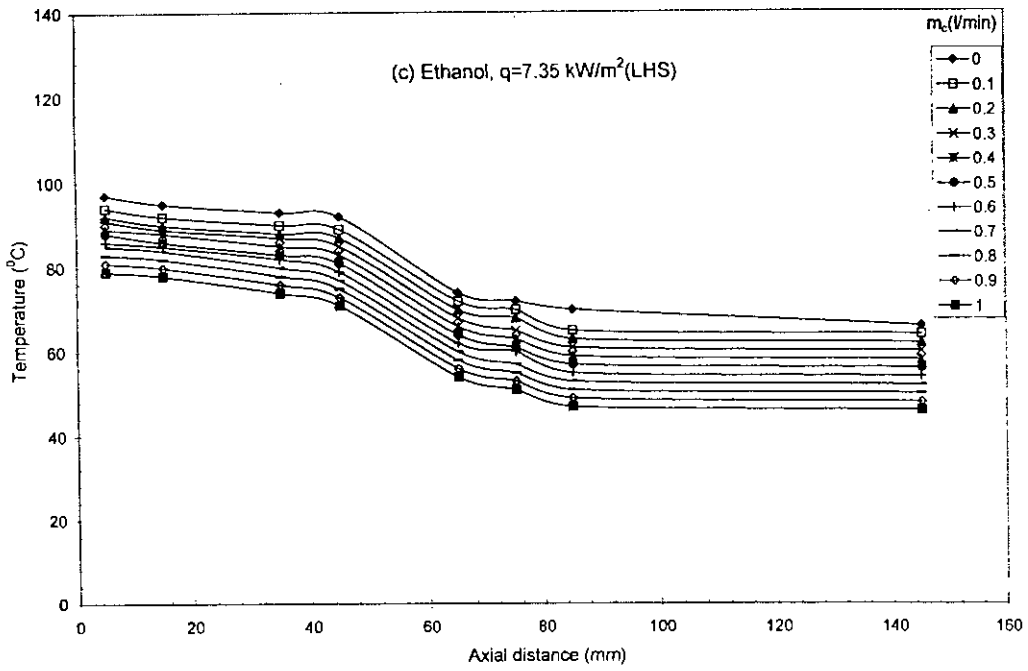


Figure 4.1.2-2 Temperature distribution for various coolant flow rate



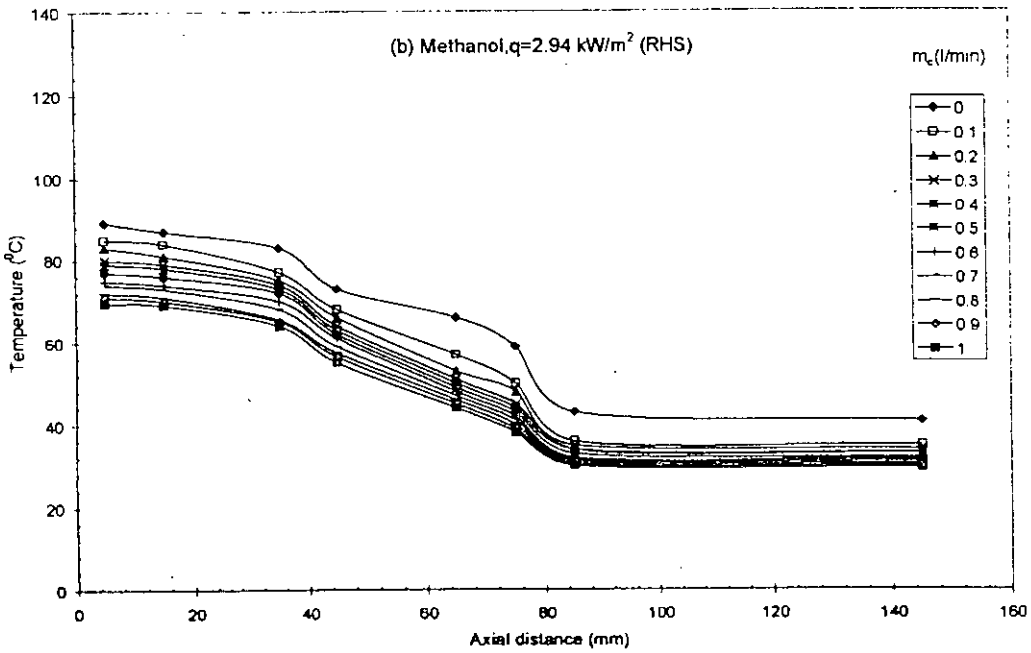
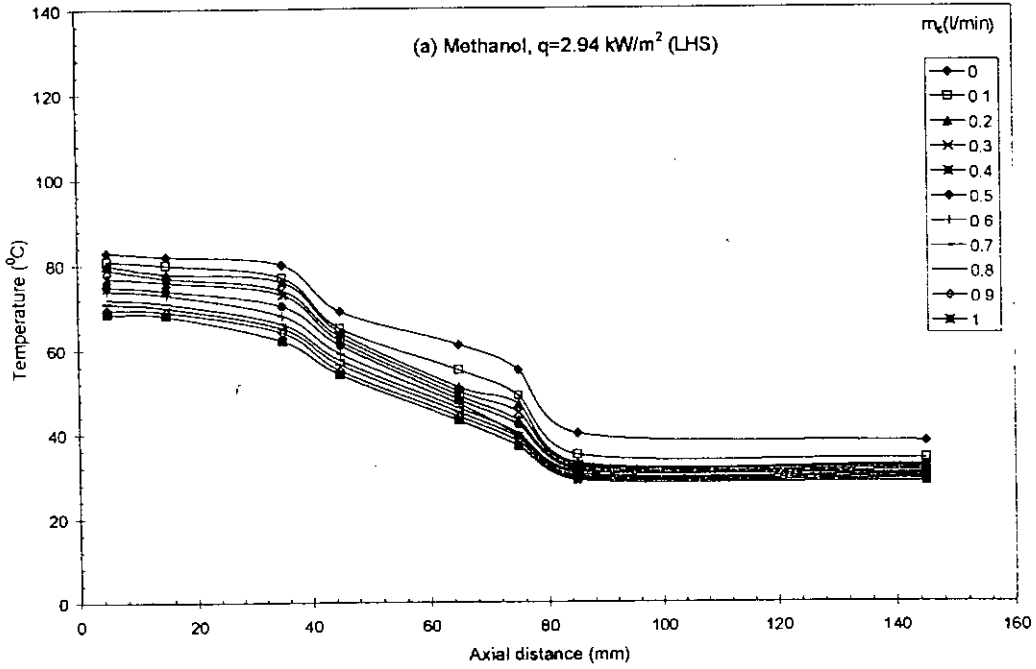


Figure 4.1.2-3 Temperature distribution for various coolant flow rate

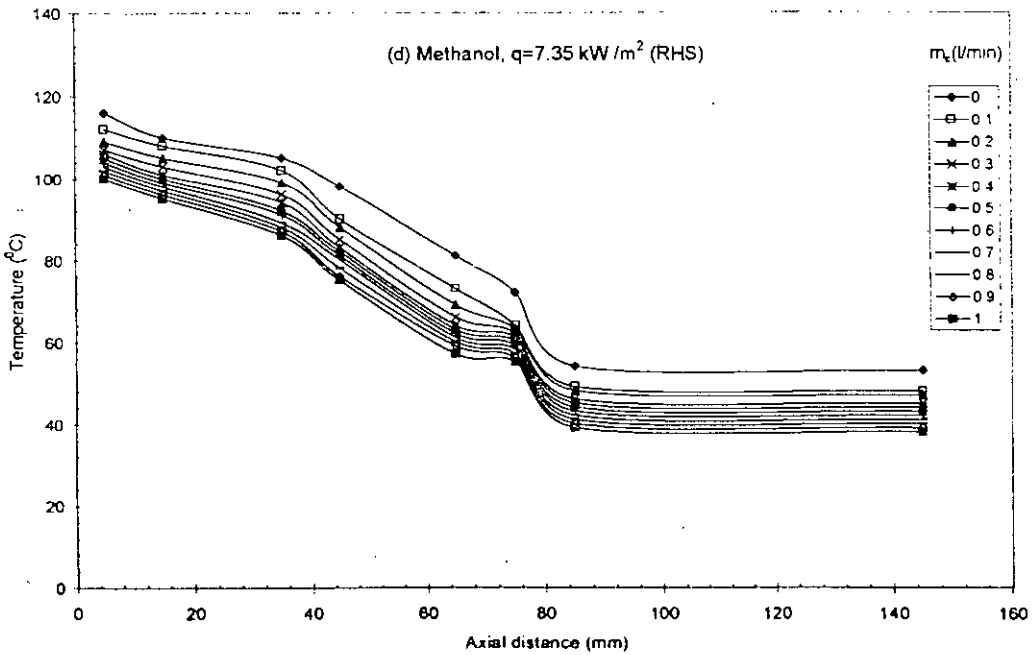
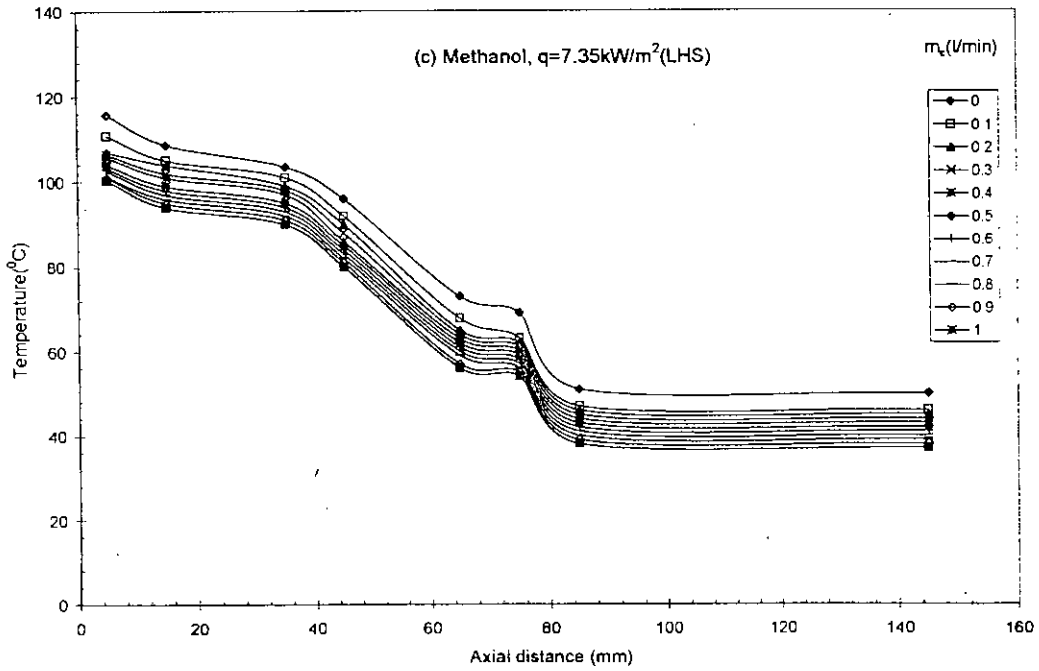


Figure 4.1.2-3 Temperature distribution for various coolant flow rate

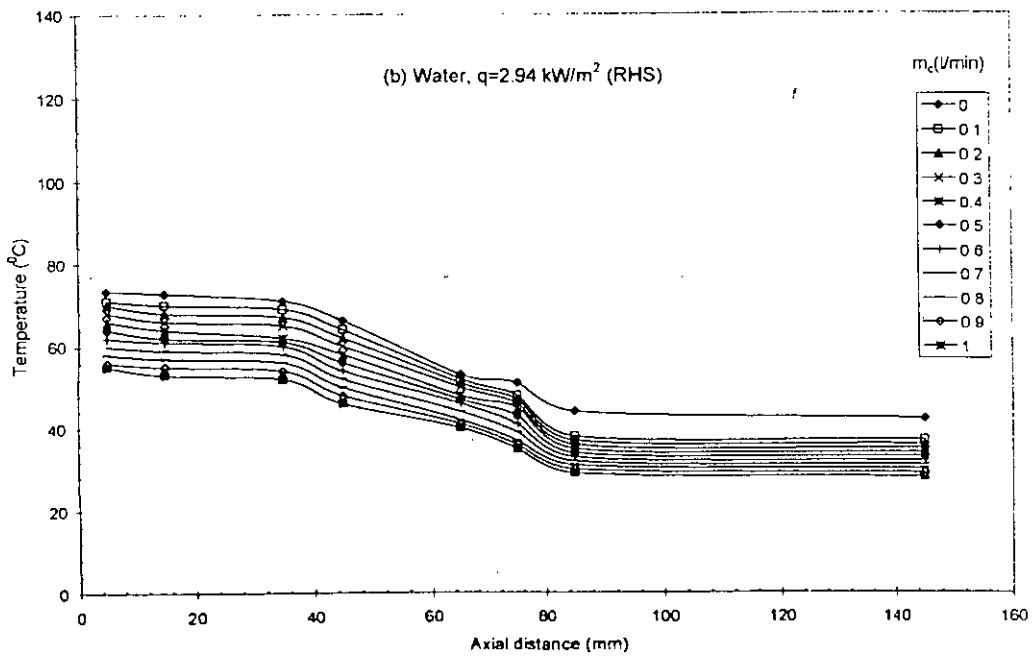
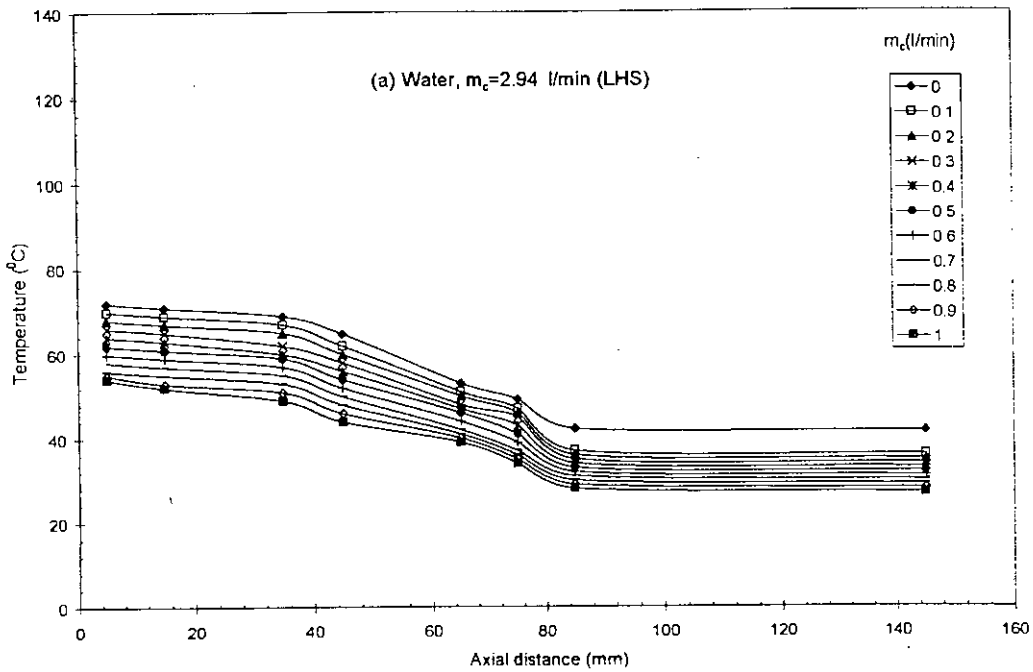


Figure 4.1.2-4 Temperature distribution for various coolant flow rate

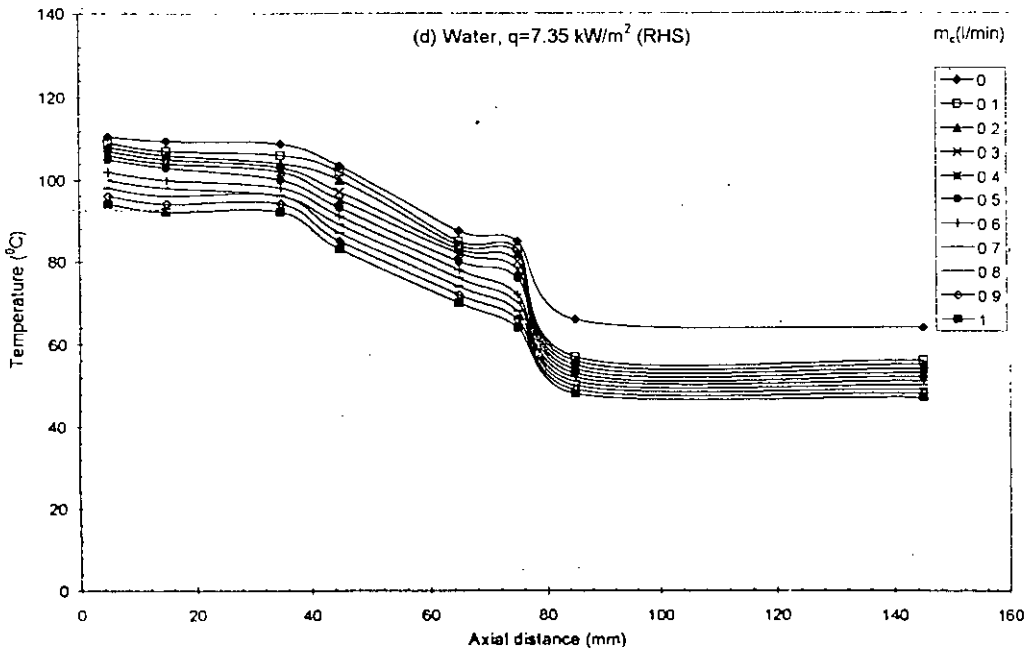
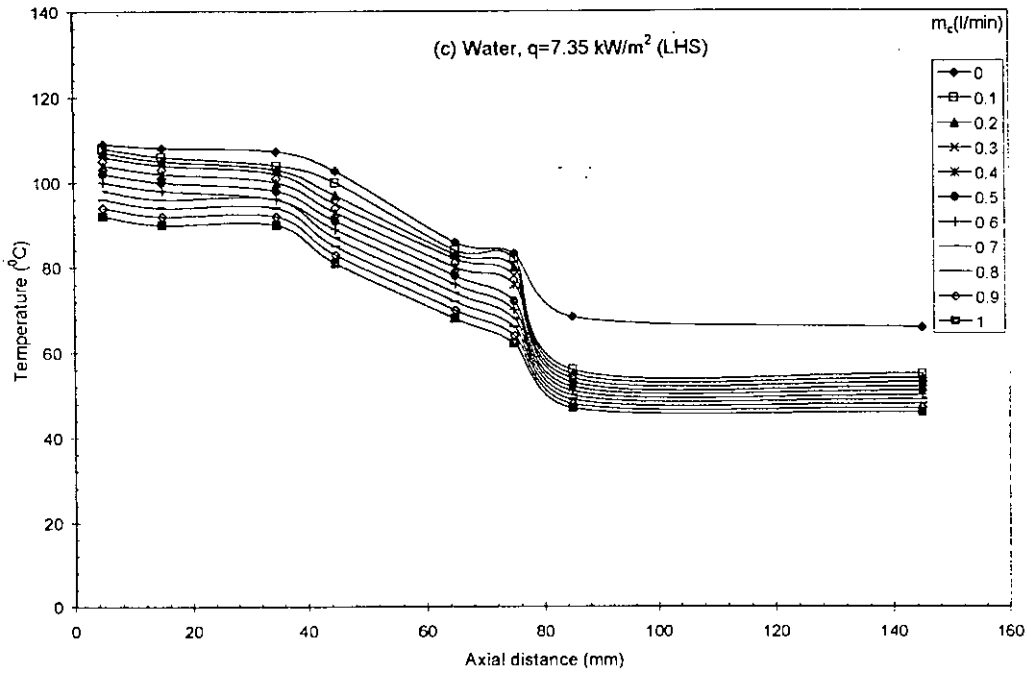


Figure 4.1.2-4 Temperature distribution for various coolant flow rate

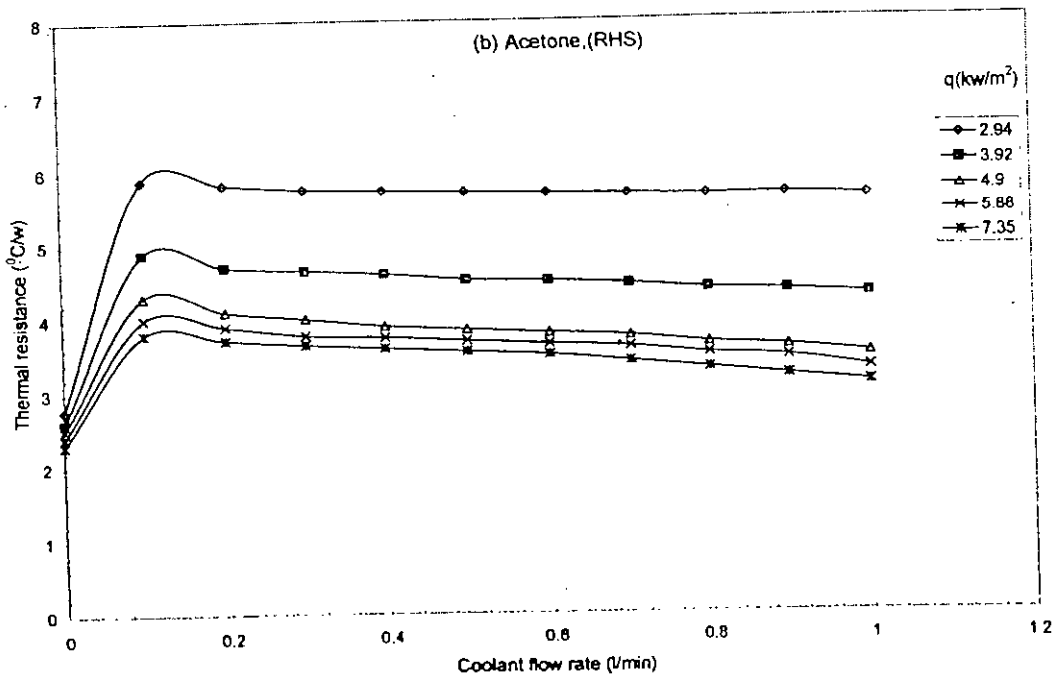
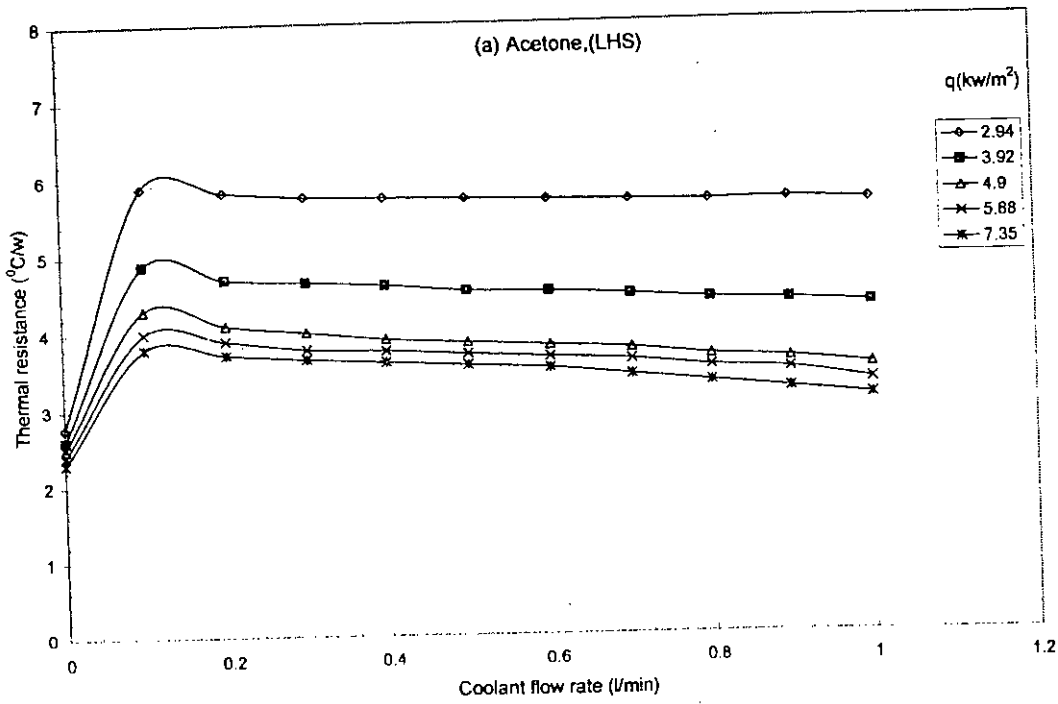


Figure 4.2.1- Effect of coolant flow rate on thermal resistance

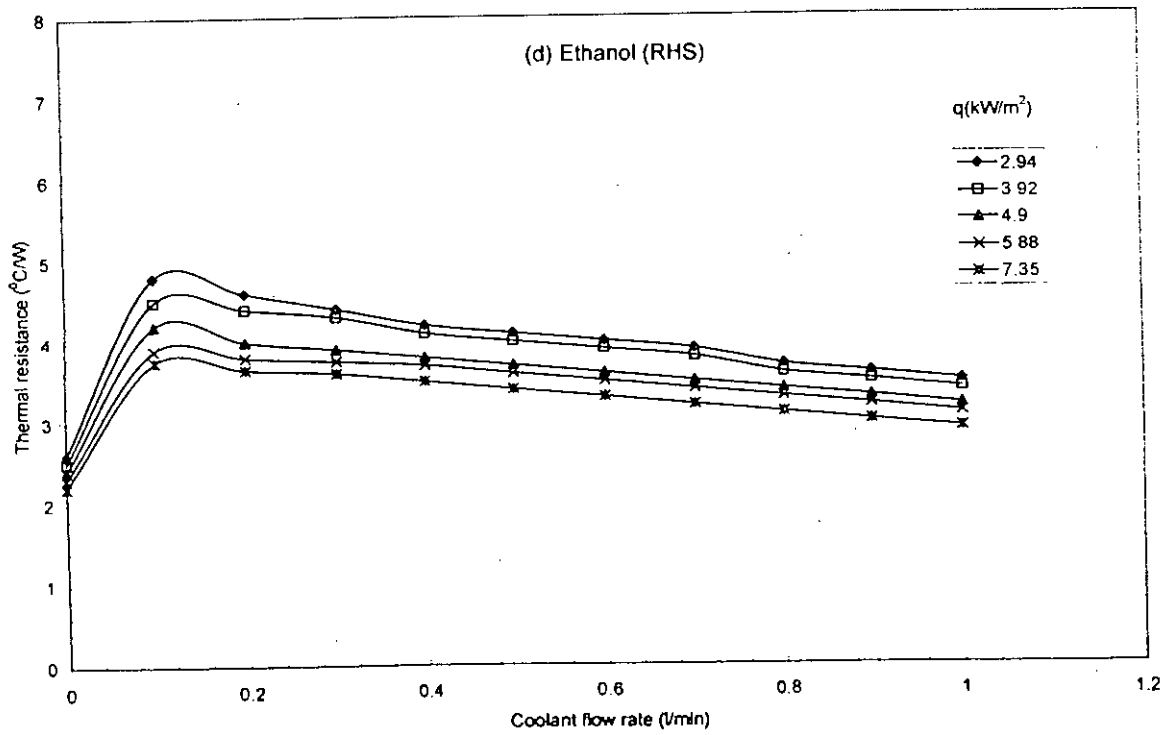
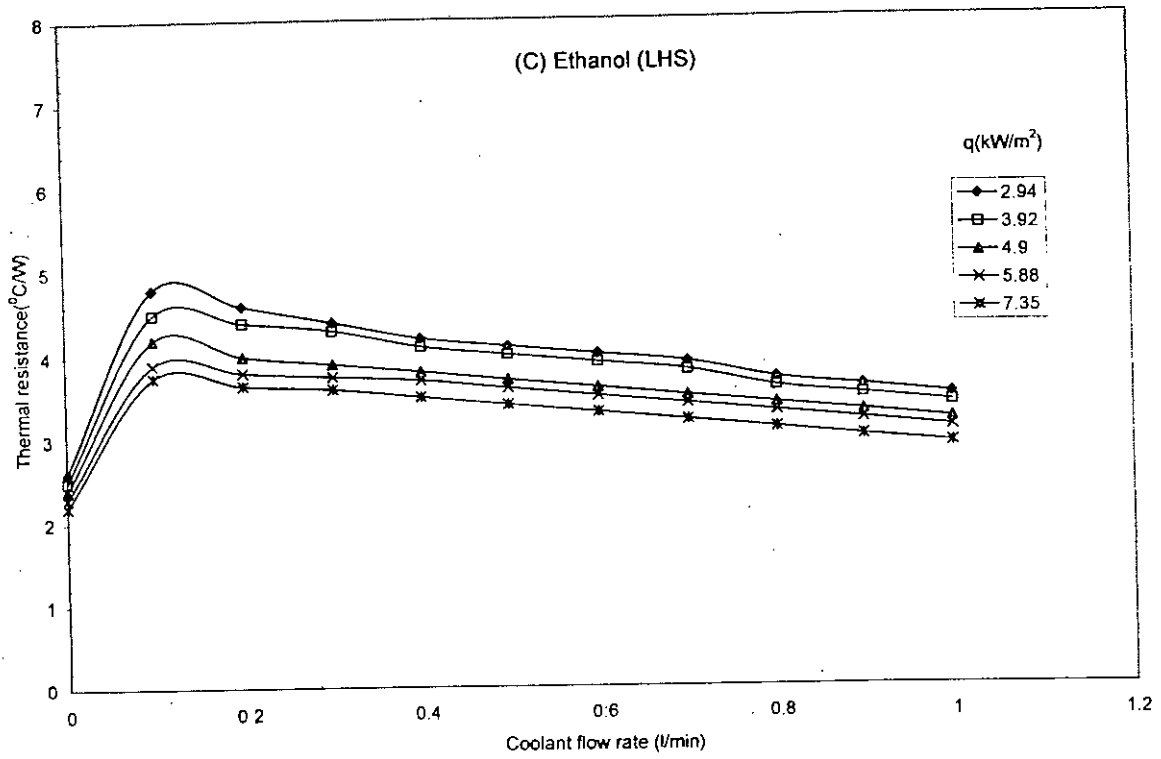


Figure 4.2.1- Effect of coolant flow rate on thermal resistance

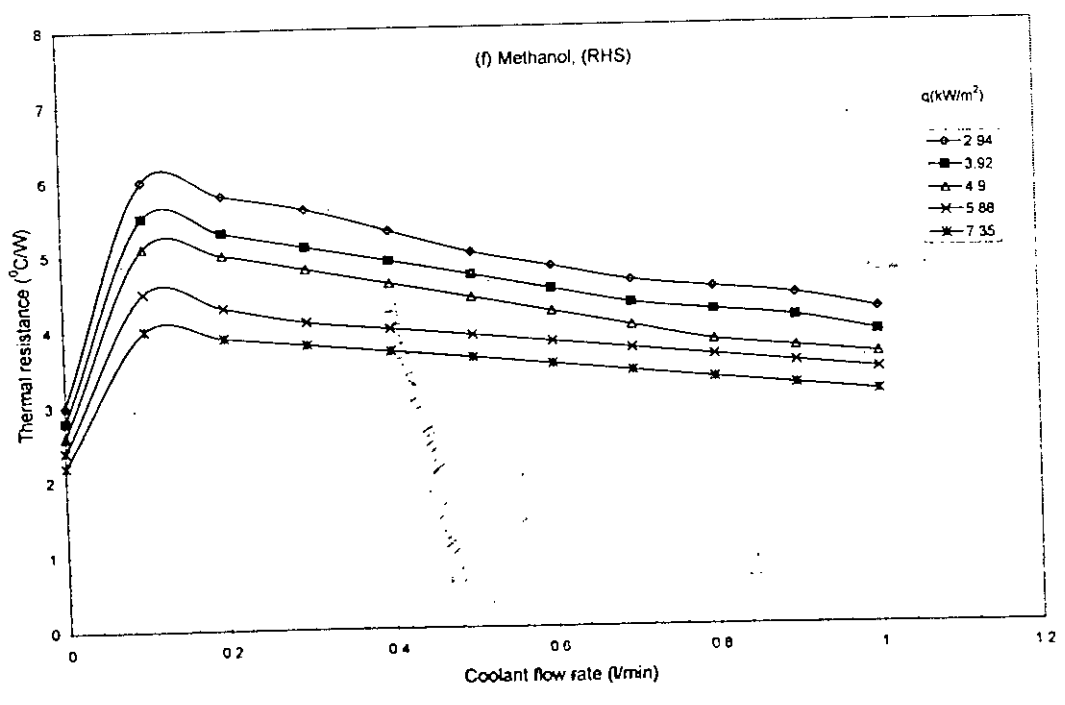
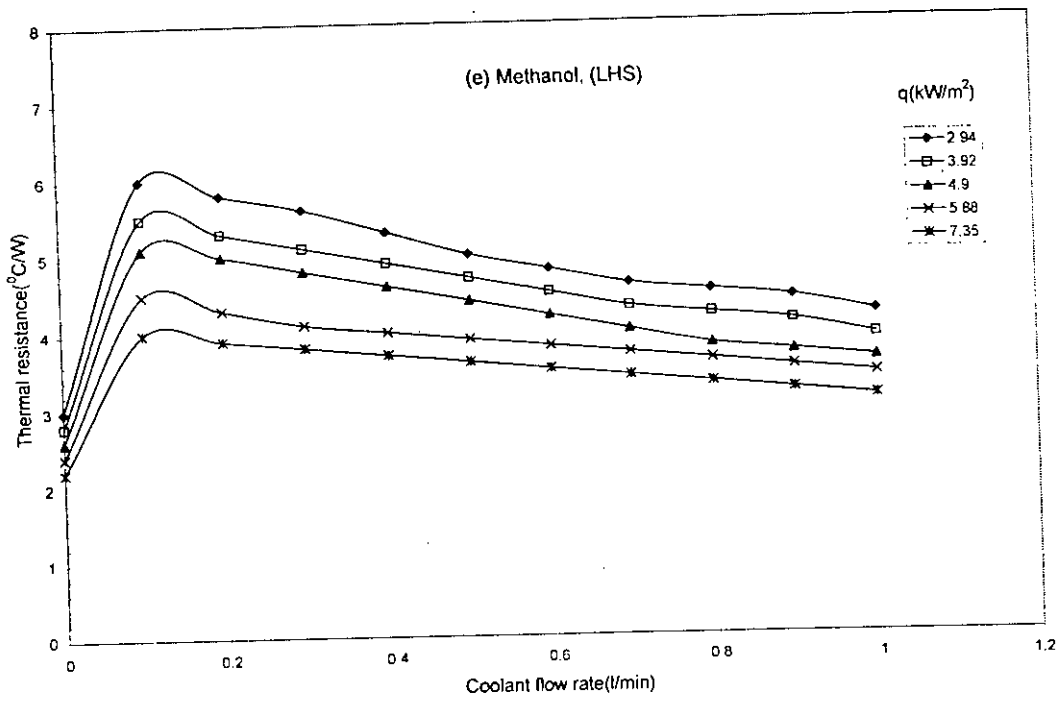


Figure 4.2.1- Effect of coolant flow rate on thermal resistance

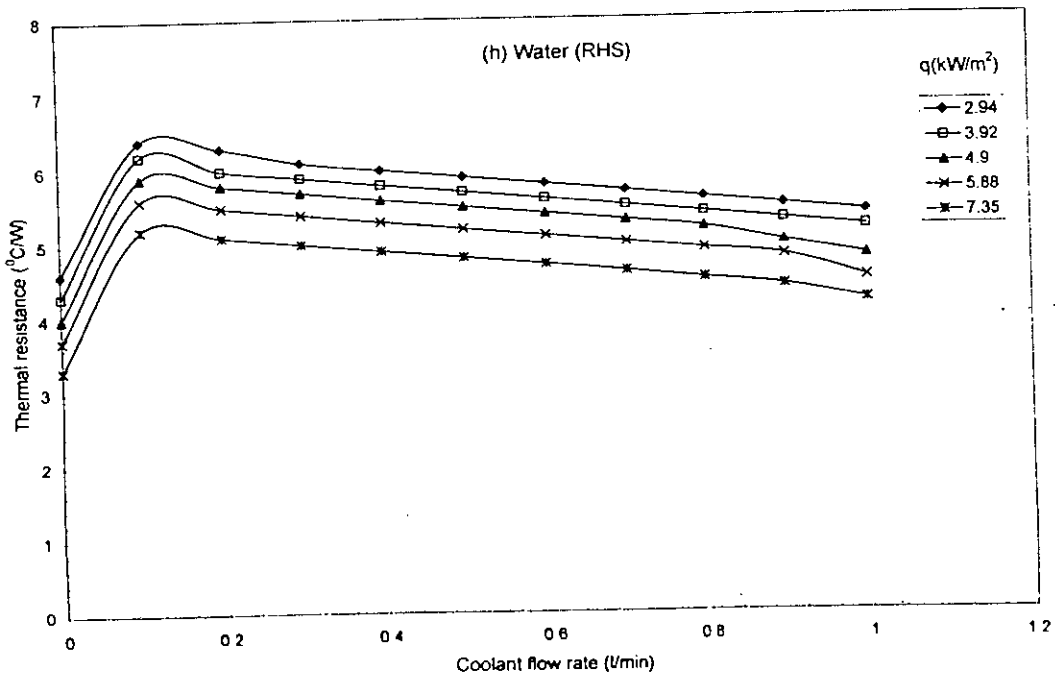
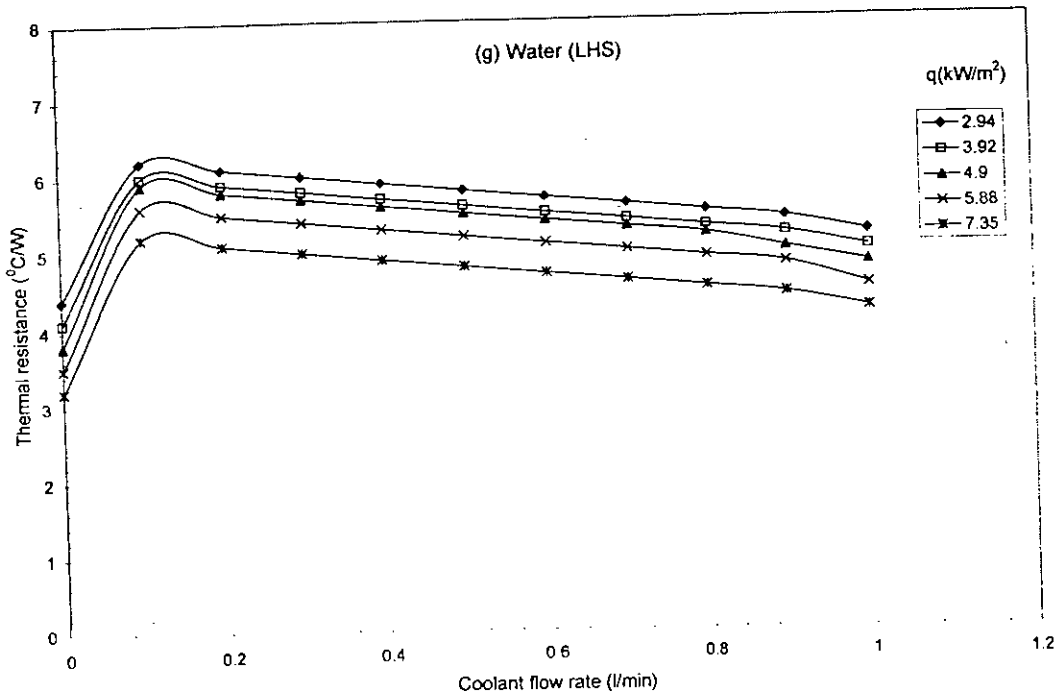


Figure 4.2.1- Effect of coolant flow rate on thermal resistance



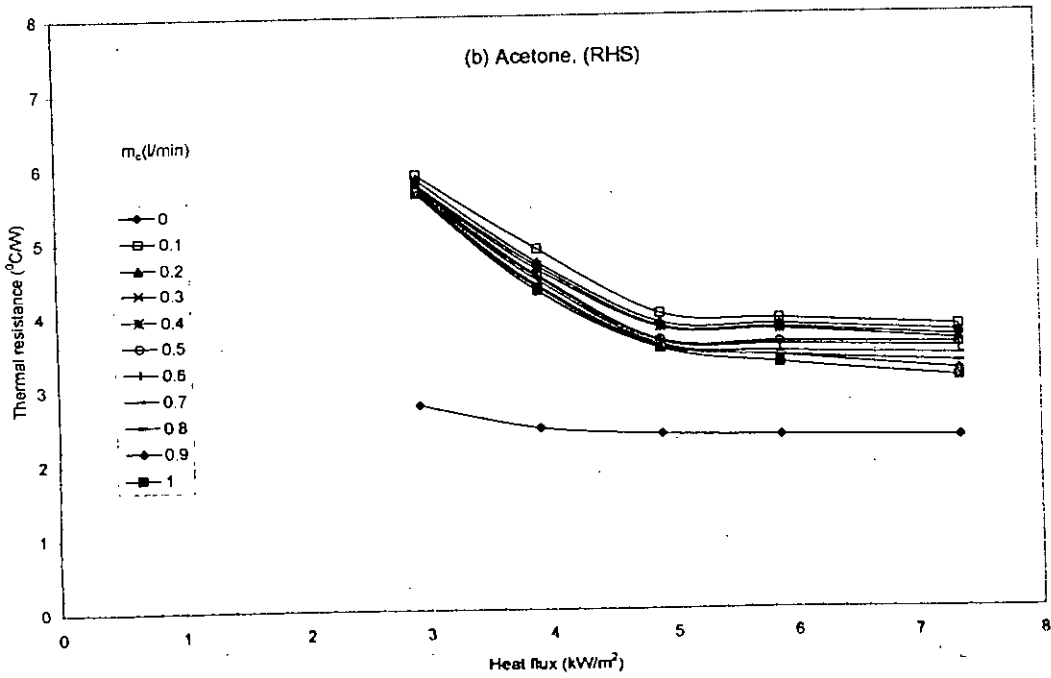
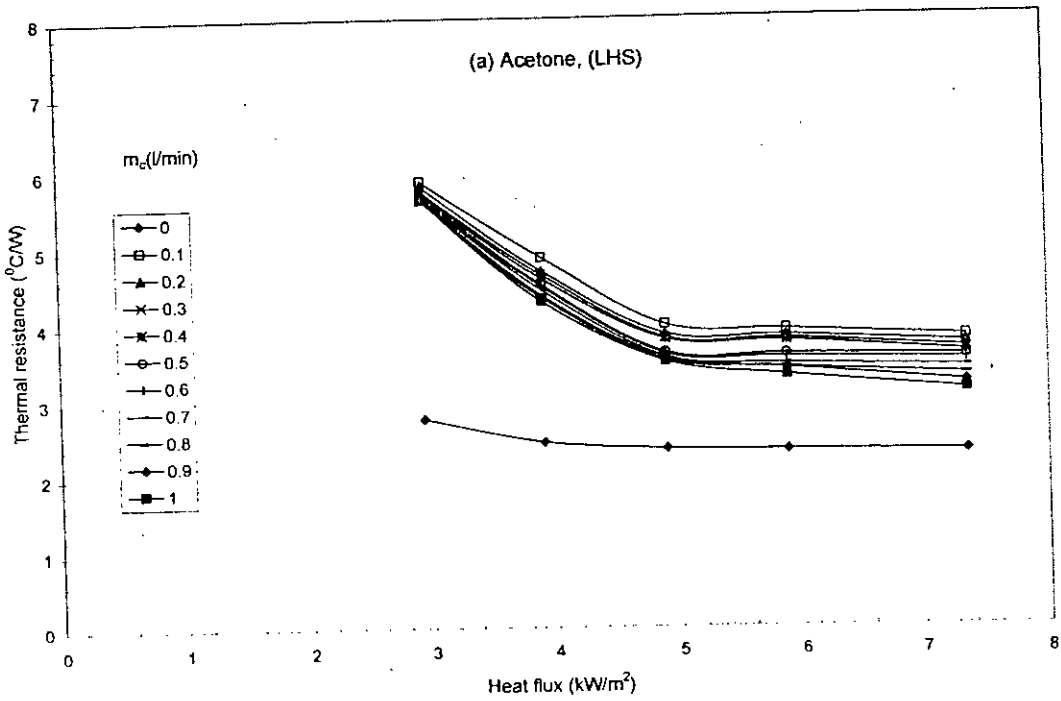


Figure 4.2.2- Effect of heat flux on thermal resistance

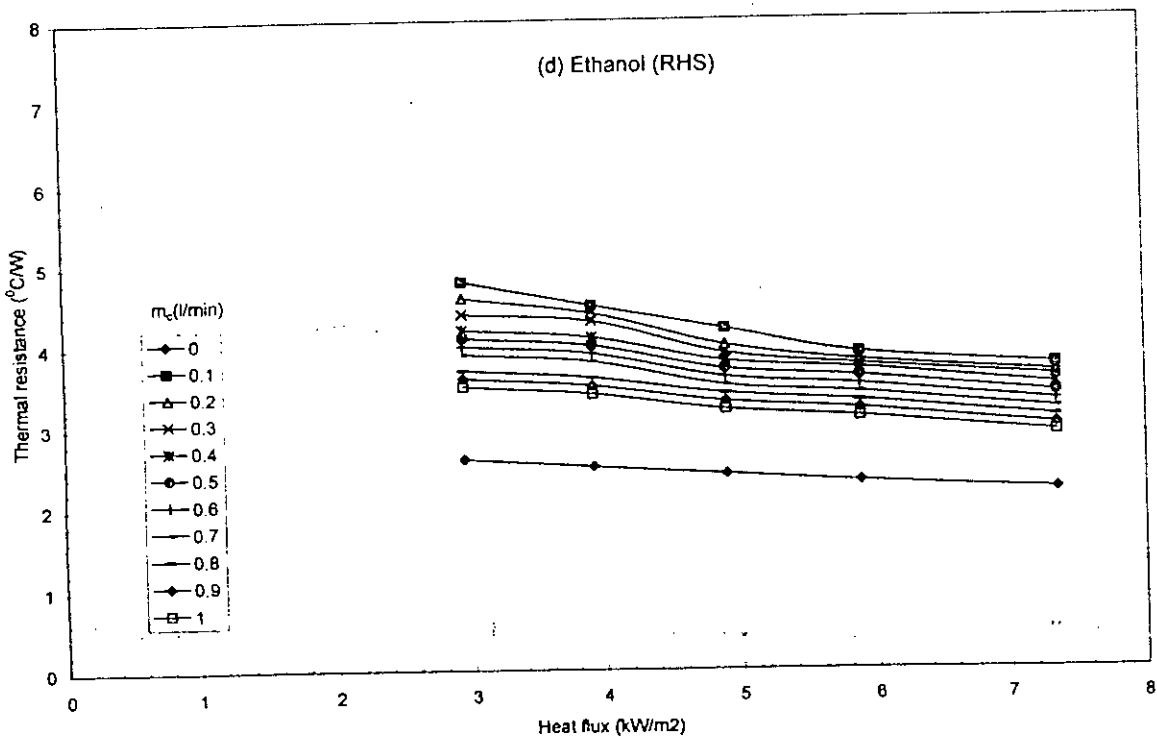
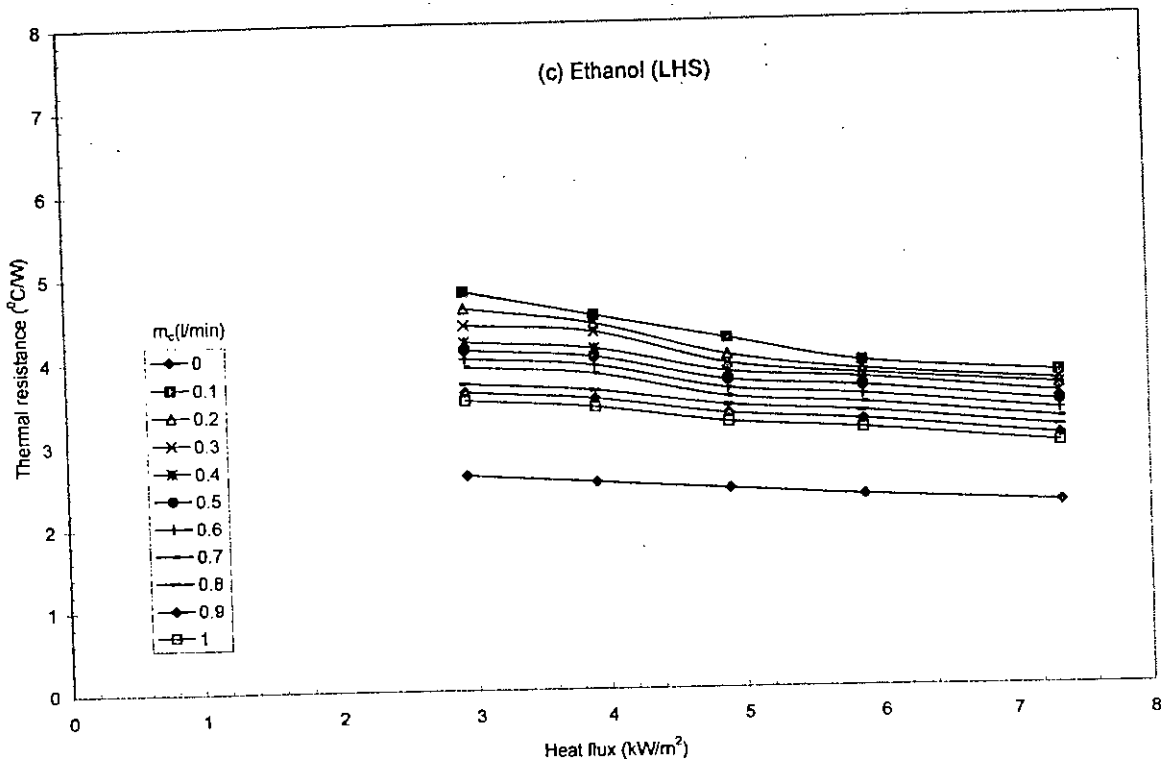


Figure 4.2.2- Effect of heat flux on thermal resistance

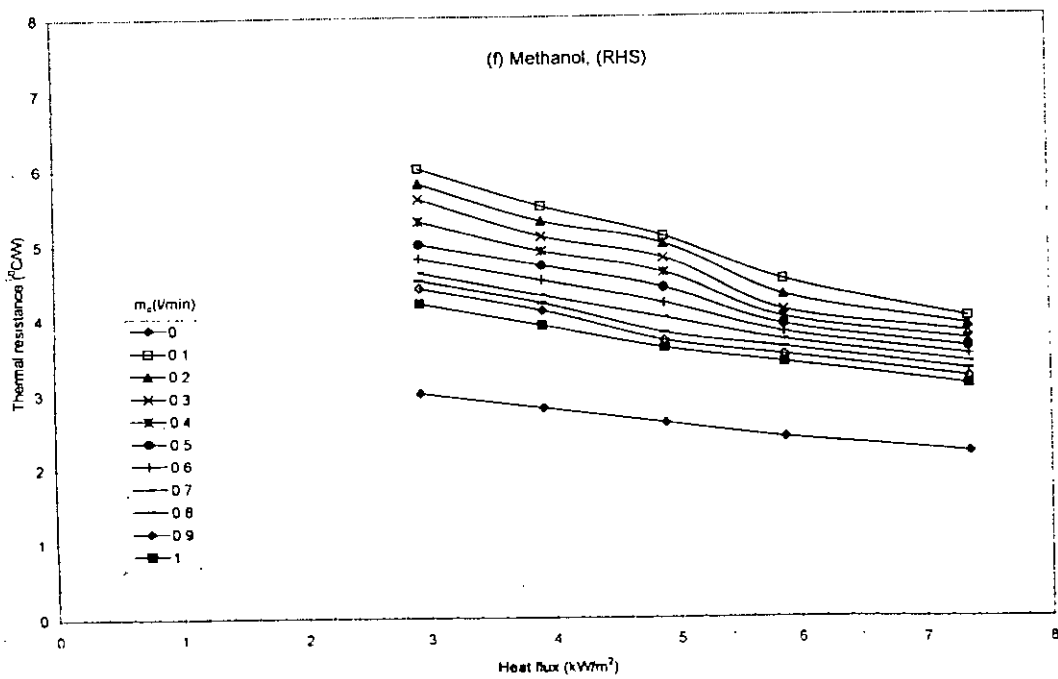
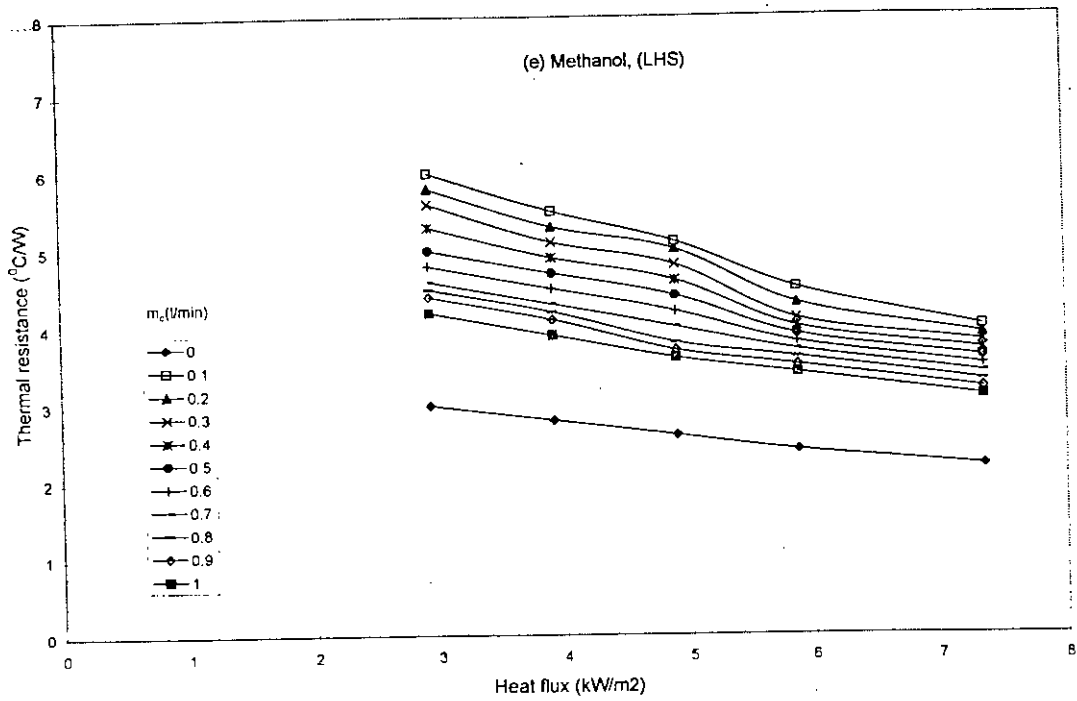


Figure 4.2.2- Effect of heat flux on thermal resistance

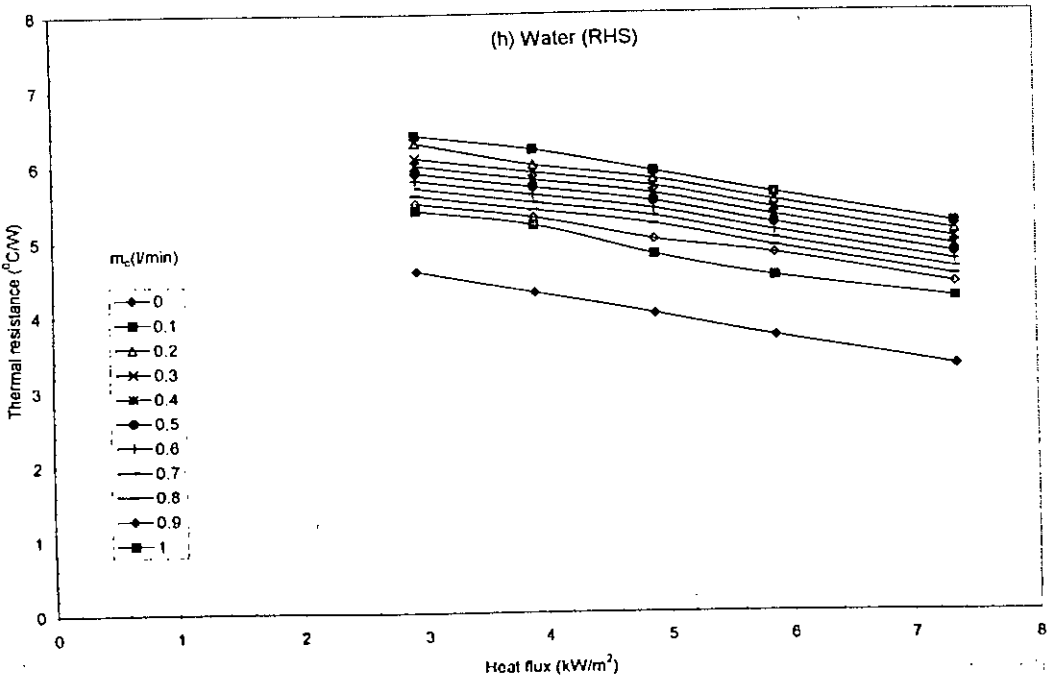
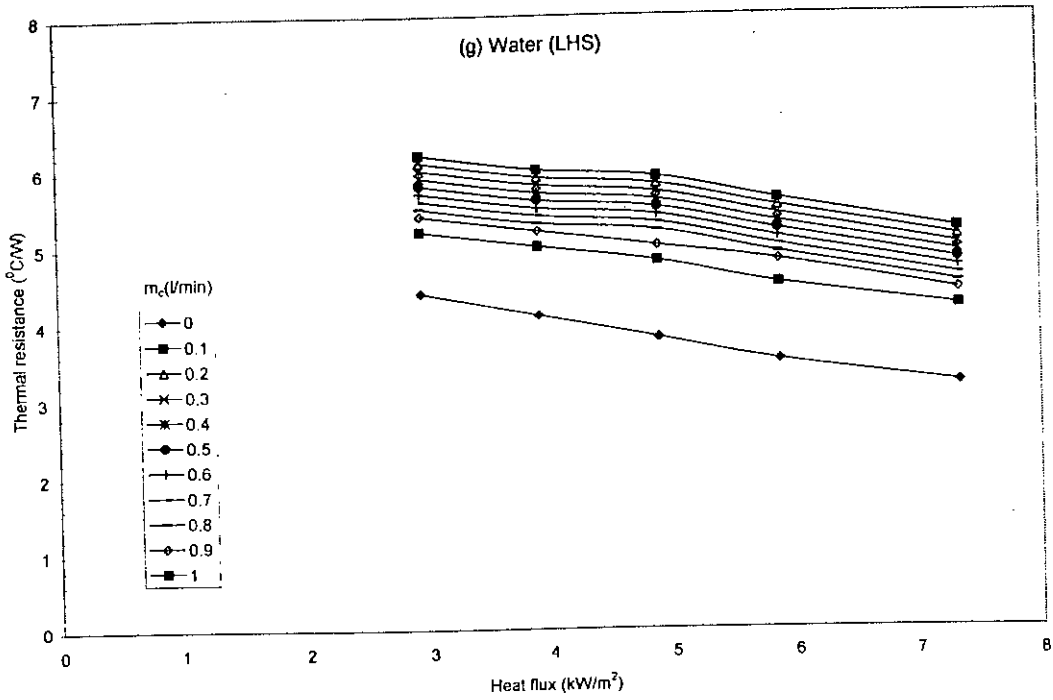


Figure 4.2.2- Effect of heat flux on thermal resistance

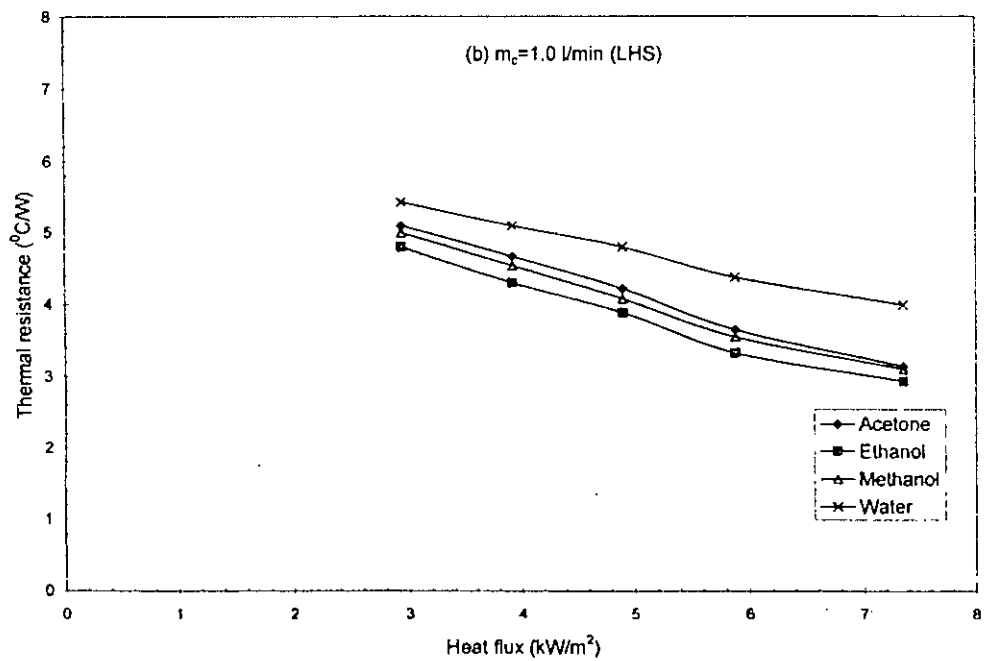
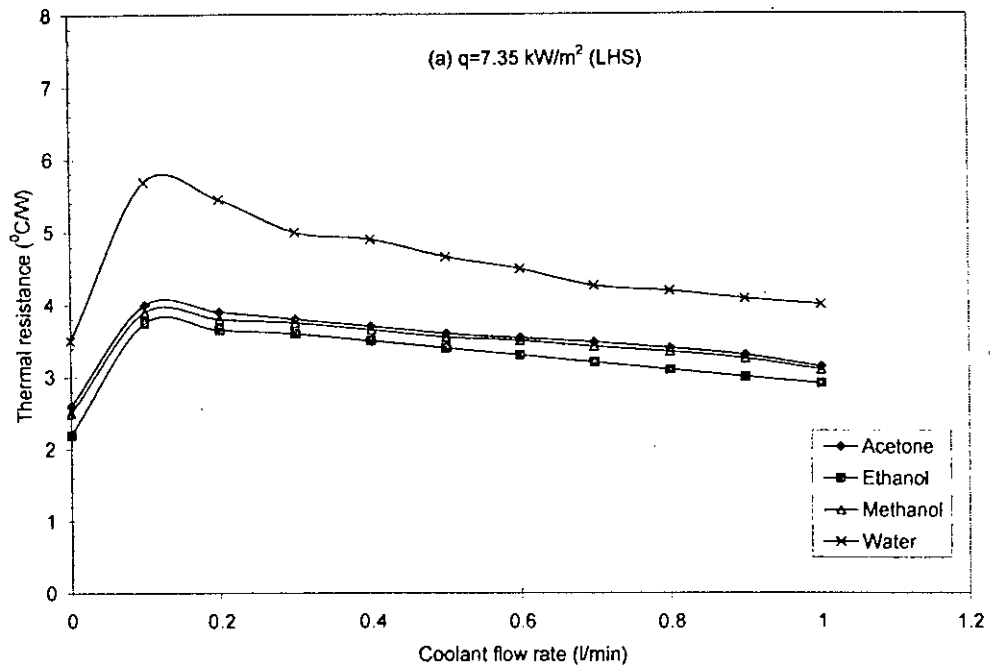


Figure: 4.3.1 Effect of working fluid on thermal resistance



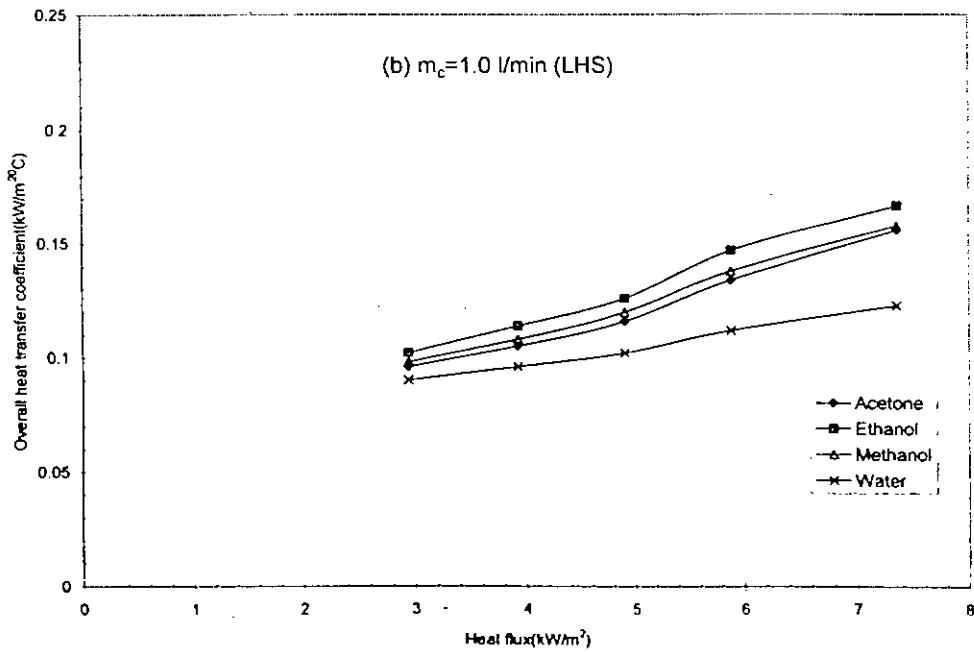
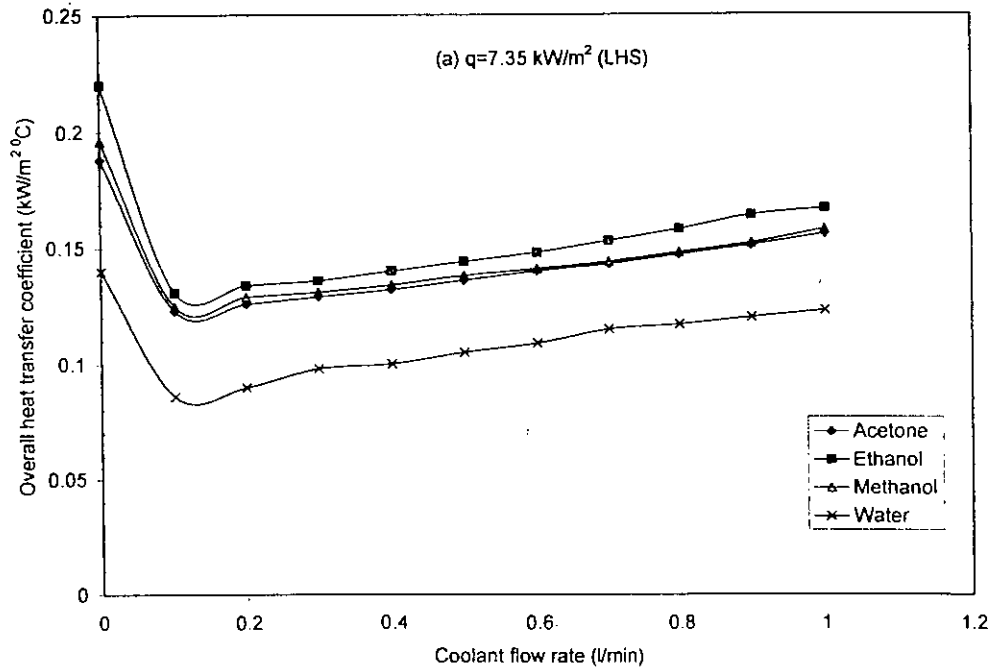


Figure: 4.3.2 Effect of working fluid on overall heat transfer coefficient

### CONCLUSIONS

The results of the performance test for the MLPT having 5.78 mm ID and length of 150 mm give the following conclusions:

- [1] The axial wall temperature of evaporator sections decreases with the increase in coolant flow rate and increases with the increase in heat flux.
- [2] The thermal resistance decreases with the increase of coolant flow rate but there is no significant change after a flow rate of 0.2 l/min for all working fluids.
- [3] Thermal resistance of the MLPT also decreases with the increase in thermal load.
- [4] Thermal resistance of ethanol is minimum and thermal resistance of water is maximum among the working fluids (ethanol, methanol, acetone and water) used in the present experimental study.
- [5] Heat transfer rate of ethanol is maximum and heat transfer rate of water is minimum among the working fluids used in the present experimental study. So ethanol shows the best performance among the working fluids.

## REFERENCES

- [1] Chowdhury, F., et al., Study on heat transfer characteristics of looped parallel thermosyphon, *Proc. 4<sup>th</sup> European Thermal science Conf.*, S10-HPI-1, 2004.
- [2] Kaminaga, F., et al., Heat transfer characteristics in an evaporator section of a looped parallel thermosyphon, *Proc. 7<sup>th</sup> International Heat pipe Symposium*, 2003, pp. 225-230.
- [3] Kim, K. S., et. al. "Cooling Characteristics Of Miniature Heat Pipes With Woven Wired Wick". pp 239 -244, proceedings of The 11<sup>th</sup> international Heat Pipe Conference – Tokyo 1999.
- [4] Luca Rossi, 'Thermal Control of Electronic equipment by Heat Pipes and Two-Phase Thermosyphons' ELBOMECC thermalloy, Via del Tipografo, 440138 Bologna, Italy.
- [5] Eguchi, K., Mochizuki, M., Mashiko, K., Goto, K., Saito, Y., Takamiya, A., Nguyen, T., "Cooling of CPU Using Micro Heat Pipe," Fujikura Co., Technical Note. Vol. 9, pp. 64~68, 1997.
- [6] Xie, H., Aghazadeh, M., Togh, J., "The Use of Heat Pipes in the Cooling of Portables with High Power Packages," Thermacore Co., Technical Note.
- [7] Mochizuki, M., Mashiko, K., Nguyen, T., Saito, Y., Goto, K., "Cooling CPU Using Hinged Heat Pipe," *Heat Pipe Technology*, Pergamon, pp. 218~229, 1997.
- [8] Kim, K. S., et. al. "Cooling Characteristics Of Miniature Heat Pipes With Woven Wired Wick". pp 239 -244, proceedings of The 11<sup>th</sup> international Heat Pipe Conference – Tokyo 1999.
- [9] Jian Ling, et. al. "Experimental Investigations of Radially Rotating Miniature High-Temperature Heat Pipes," *ASME Journal*, 2001.
- [10] Lanchao Lin et. al "High Performance Miniature Heat Pipes," *Thermal Management Research Studies*. Volume 1. Page-86.
- [11] Amir Faghri et. al. "Micro/ Miniature Heat pipe Analysis" *Springer Media*, Page –175.
- [12] Jun Zhuang et. al. "Comparison of Heat Transfer Performance Of Miniature Heat Pipes." pp.226~229, proceedings of The 11<sup>th</sup> International Heat Pipe Conference- Tokyo 1999.
- [13] Thang Nguyen et. al. "Prediction of long-term performance of Miniature Heat Pipe from Accelerated Life tests," pp.230~233, proceedings of The 11<sup>th</sup> International Heat Pipe Conference- Tokyo 1999.



# APPENDIX

## APPLICATION OF THERMOSYPHON

Thermosyphons have found numerous applications. Today thermosyphons are widely used in computers, electronics equipments and various other applications. Now typical applications of thermosyphons are presented below:

- a. Stirling cycle cooled domestic refrigerator
- b. Effect of electric field on heat transfer performance of automobile radiator at low front area velocity
- c. Miniature pulsated loop thermosyphon for desktop computer cooling

### **a. Stirling cycle cooled domestic refrigerator**

A closed looped thermosyphon system was constructed by connecting a heat exchanger which was placed on the cold head of the stirling cooler directly to another heat exchanger placed in the cabinet as evaporator. On the other hand, since effective heat transfer is needed on the warm head to obtain efficient operating conditions an extended surface aluminum heat exchanger was placed on the warm head of the cooler and a fan was used to obtain forced convection heat transfer. The prototype refrigerating unit was tested for different charge quantities of the refrigerant filled in the thermosyphon loop as well as different input voltages of the cooler. The temperature of the key points on the cold side thermosyphon, the temperatures of the shelves of the cabinet and the input power of the stirling cooler were recorded. Figure.1 and figure.2 show stirling cycle cooled domestic refrigerator .

### **b. Effect of electric field on heat transfer performance of automobile radiator at low front area velocity**

Automobile radiator, one type of cross flow heat exchanger, is an important part of vehicle engine. Normally, it is used as a cooling unit of the engine and the water is heat transfer medium.

Fig. 3 shows automobile radiator at low front area velocity. An automobile radiator is mounted in a wind tunnel and there is heat exchange between hot water flowing in the tube-side and air stream flowing across the heat exchanger. Note that, the velocity of the air stream is measured by a standard nozzle and controlled by a frequency inverter which controls the air blower speed. The inlet and the outlet temperatures of the air and the hot water at the automobile radiator are measured by a set of K-type thermocouples. The flow rate of the hot water is measured by a flow meter. The inlet temperature of water is controlled by a temperature controller. A set of parallel

electrodes is installed in front of the automobile radiator. The frontal velocity of the air stream is varied from 0.5 to 2.1 m/s. The inlet temperature of the air is 25 °C. The flow rate and the inlet temperature of the water are kept constant at 20 l/min and 75 °C, respectively. The supply voltage of the electric field is controlled by a high voltage generator and it is varied from 0 to 12 kV.

### **c. Miniature pulsated loop thermosyphon for desktop computer cooling**

A generic pulsated two phase thermosyphon (PTPT) consists of an evaporator, a condenser anyway located respect to the gravity and an accumulator, separated from the evaporator. The evaporator is connected with the condenser through a vapour line and with the accumulator through a liquid return line. The line connecting the condenser with the accumulator is named liquid line. Two check valves drive the flow in a fixed direction. PTPT device is used for electronic equipments cooling and for desktop computer. Figure 4 shows functioning of a PTPT. The delaying tank has been realized into the evaporator volume. The electronic components are substituted with a cylindrical copper dissipator heated with a thermoelectric heater at the bottom. The copper dissipator has been studied with a finite elements commercial code to investigate on its temperature distribution uniformity and on the heat power dissipation rate from the lateral surface, which results lower than 5%. Its flat heat exchange surface is 3.14 cm<sup>2</sup>. In order to keep low the average temperature of the aluminum walls of the evaporator, the copper dissipator has been thermally disconnect to them. The delaying tank and the evaporator are connected with a glass hydrosyphon, and are monitored by 5 thermocouples and a pressure gauge. The condenser is aluminium made and consists of a flat plate 64 x 78 mm sized and 8 mm thick with 22 rectangular fins 28 mm high, 78 mm long and 1.3 mm thick. Figure 5 shows Miniature pulsated loop thermosyphon for desktop computer cooling.

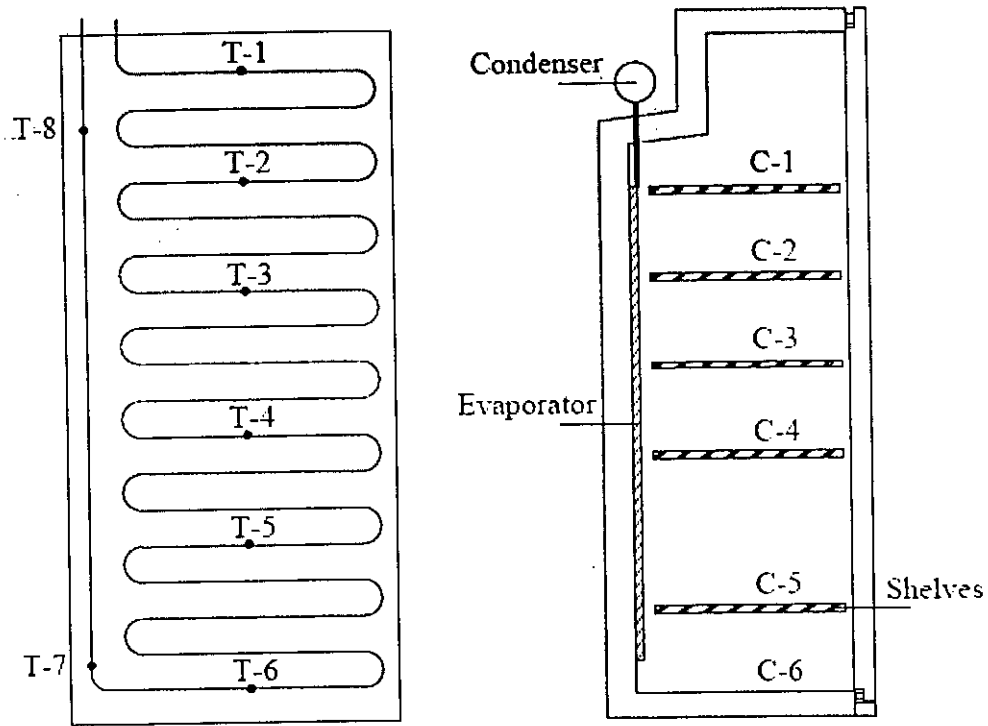


Figure 1.a : Schematic of the evaporator of the thermosyphon system.  
 Figure 1.b : Upside-down cabinet, location of the evaporator, condenser and the shelves.

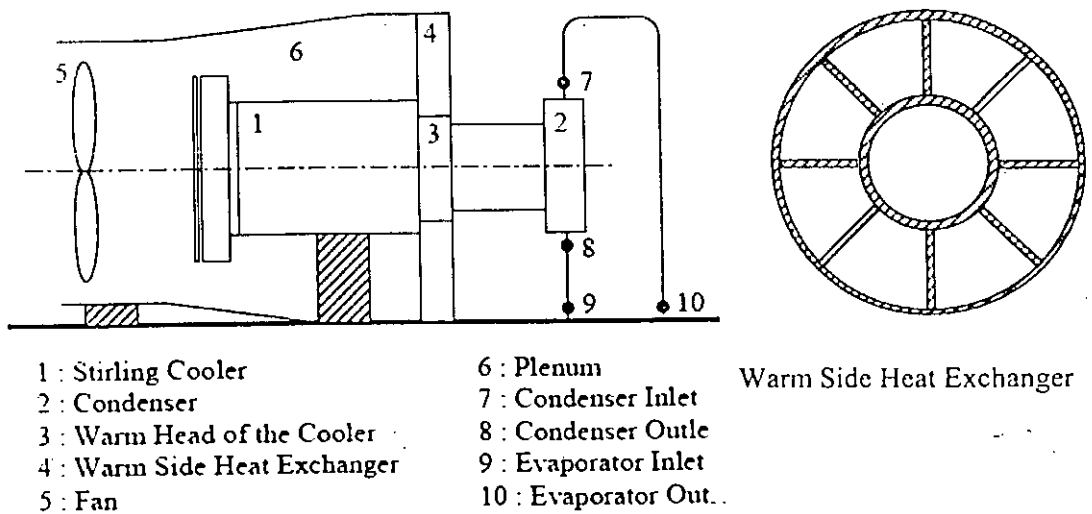


Figure 2 : Stirling cycle cooled domestic refrigerator

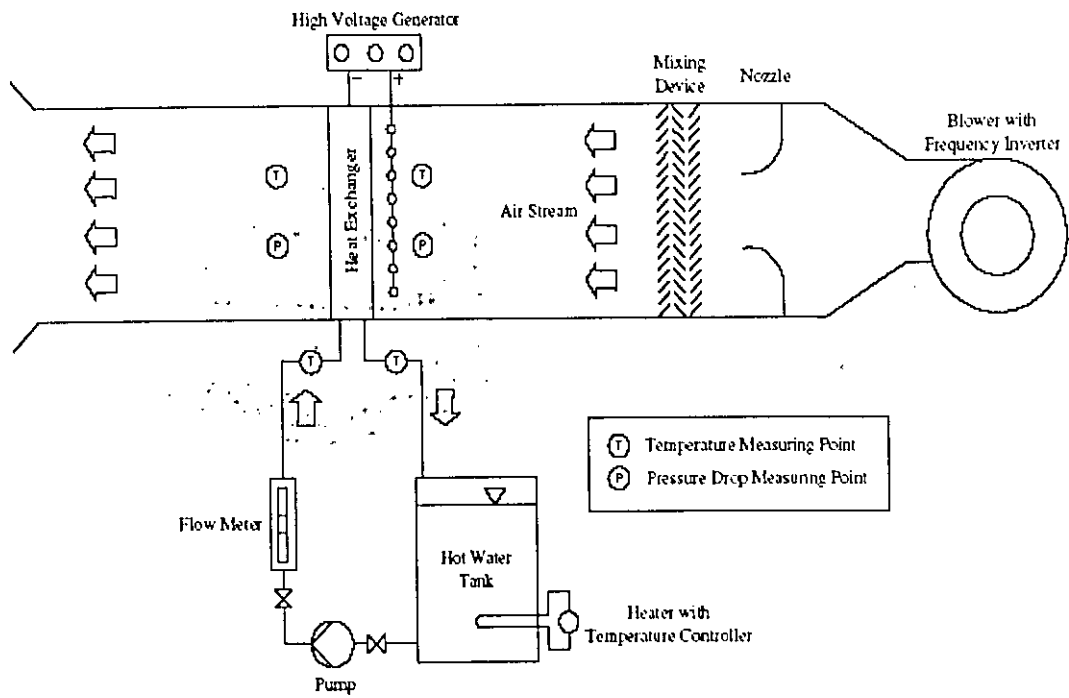


Fig. 3: The schematic sketch of automobile radiator at low front area velocity.

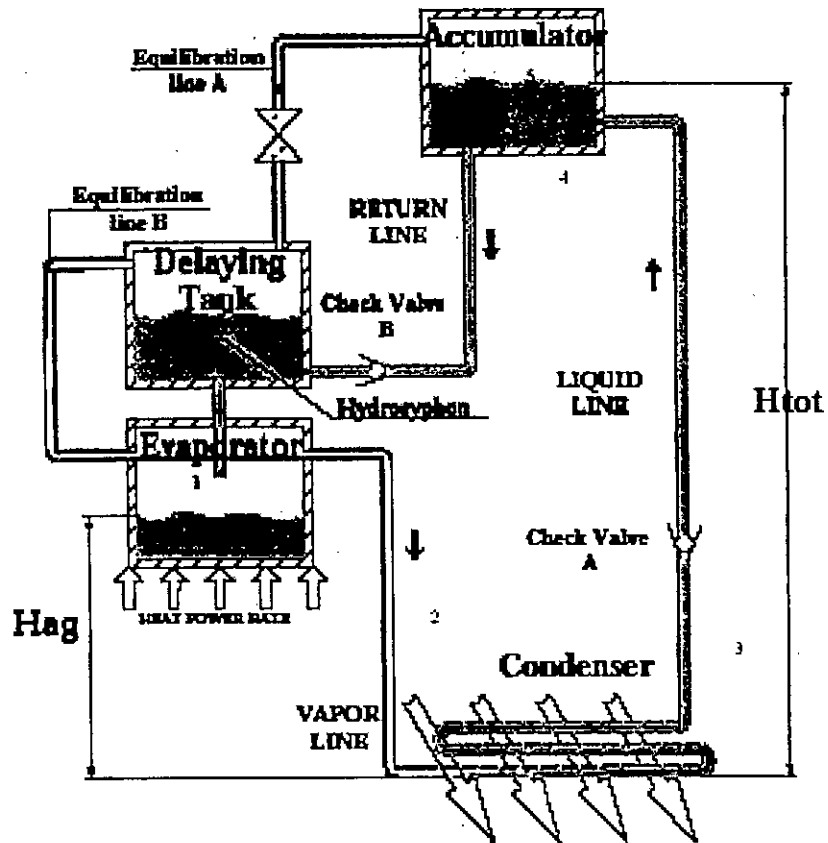


Figure 4– Functioning scheme of a pulsated two phase thermosyphon (PTPT).



Figure 5 – Miniature pulsated loop thermosyphon for desktop computer cooling